Synthesis, mechanisms of action, and toxicity of novel aminophosphonates derivatives conjugated irinotecan *in vitro* and *in vivo* as potent antitumor agents

Xiaochao Huang, Meng Wang, Qinghong You, Jing Kong, Haijiang Zhang, Chunhao Yu, Yanming Wang, Hengshan Wang, Rizhen Huang

PII: S0223-5234(20)30034-9

DOI: https://doi.org/10.1016/j.ejmech.2020.112067

Reference: EJMECH 112067

To appear in: *European Journal of Medicinal Chemistry*

Received Date: 17 October 2019

Revised Date: 10 January 2020

Accepted Date: 12 January 2020

Please cite this article as: X. Huang, M. Wang, Q. You, J. Kong, H. Zhang, C. Yu, Y. Wang, H. Wang, R. Huang, Synthesis, mechanisms of action, and toxicity of novel aminophosphonates derivatives conjugated irinotecan *in vitro* and *in vivo* as potent antitumor agents, *European Journal of Medicinal Chemistry* (2020), doi: https://doi.org/10.1016/j.ejmech.2020.112067.

Graphical abstract

Synthesis, mechanisms of action, and toxicity of novel aminophosphonates derivatives conjugated irinotecan *in vitro* and *in vivo* as potent antitumor agents

Xiaochao Huang [a, b, c 1*], Meng Wang [a 1], Qinghong You [a], Jing Kong [a], Haijiang Zhang [a], Chunhao Yu [a], Yanming Wang [a], Hengshan Wang [c *] and Rizhen Huang [b*]

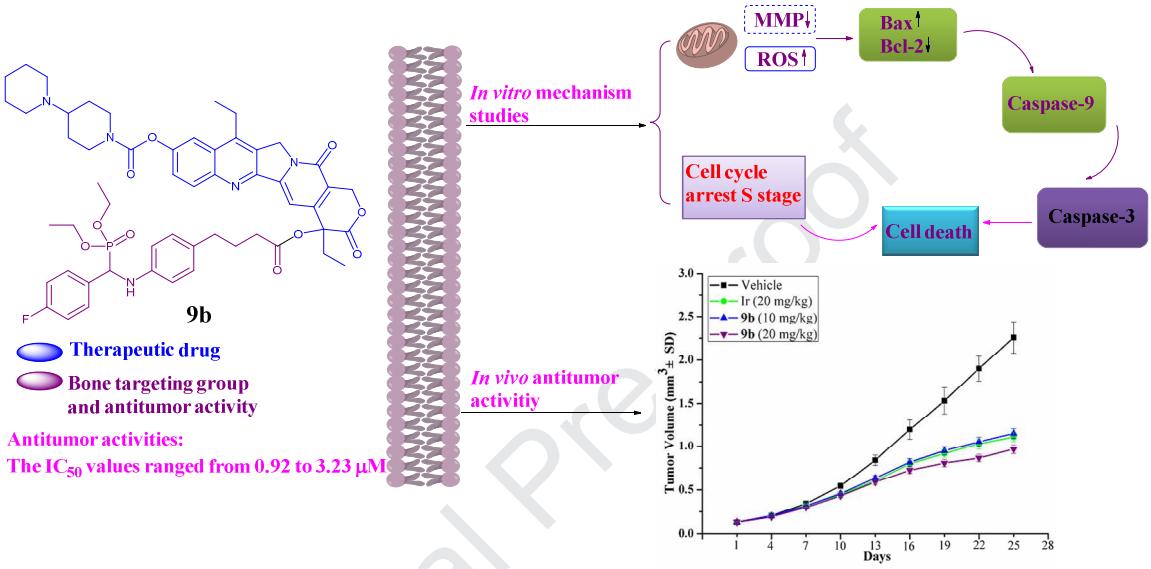

Synthesis, mechanisms of action, and toxicity of novel aminophosphonates derivatives conjugated irinotecan *in vitro* and *in vivo* as potent antitumor agents

Xiaochao Huang [a, b, c 1*], Meng Wang [a 1], Qinghong You [a], Jing Kong [a], Haijiang Zhang [a], Chunhao Yu [a], Yanming Wang [a], Hengshan Wang [c *] and Rizhen Huang [b*]

[a] Jiangsu Key Laboratory of Regional Resource Exploitation and Medicinal Research, Huaiyin Institute of Technology, Huaian 223003, China.

[b] College of biotechnology, Guilin Medical University, Guilin 541004, China.

[c] State Key Laboratory for the Chemistry and Molecular Engineering of Medicinal Resources, School of Chemistry and Pharmaceutical Sciences of Guangxi Normal University, Guilin 541004, China.

Abstract

Twenty novel aminophosphonates derivatives (**5a-5j and 6a-6j**) conjugated irinotecan were synthesized through esterification reaction, and evaluated their anticancer activities using MTT assay. *In vitro* evaluation revealed that they displayed similar or superior cytotoxicity compared to the positive drug irinotecan against A549, MCF-7, SK-OV-3, MG-63, U2OS and multidrug-resistant (MDR) SK-OV-3/CDDP cancer cell lines. Among them, **9b** displayed the most potent activity, with IC_{50} values of 0.92-3.23 μM against five human cancer cells, which exhibited a 5.4~19.1-fold increase in activity compared to the reference drug irinotecan, respectively. Moreover, cellular mechanism studies suggested that **9b** arrested cell cycle at S stage and induced cell apoptosis along with the decrease of mitochondrial membrane potential (MMP). Interestingly, **9b** significantly inhibited tumor growth in SK-OV-3 xenograft models *in vivo* without apparent toxicity, which was better than the positive drug irinotecan. Taken together, **9b** possessed potent antitumor activity and may be a promising candidate for the potential treatment of human ovarian cancer cells.

Keywords: Irinotecan; Aminophosphonate ester; Anti-tumor activity; Apoptosis

* Corresponding author.

E-mail addresses: viphuangxc@126.com; whengshan@163.com; rzhuang1783@163.com.

[1] Co-first author: These authors contributed equally to this work.

1. Introduction

It is well known that malignant tumor has become one of the most important causes of death worldwide due to its high rates of morbidity and mortality [1, 2]. Therefore, how to treat malignant tumor is a huge challenge for modern medicine technology. Currently, among various cancer treatments, the main method was still used chemotherapy owing to its high efficiency. However, the conventional chemotherapy usually suffered from several limitations, such as nonspecific selectivity, poor bioavailability, severe drug resistance, and severe adverse reaction for healthy tissues [3-5]. Increasing evidence indicated that targeted drug design is one of the most promising strategies to improve drug accumulation in tumors and therapeutic efficacy as well as reduce drug toxicity.

Camptothecin (CPT) and its analogs irinotecan (Ir) and 10-Hydroxy camptothecin (SN-38), as a well-known topoisomerase I (Topo I) inhibitors (**Fig. 1**), are widely used for cancer chemotherapy [6-9]. Most commonly, irinotecan can not only be used in combination with fluorouracil (5-FU) and leucovorin (LV) as a first-line treatment option for metastatic colorectal cancer patients but also can serve as a monotherapy for colorectal cancer patients [10, 11]. However, the poor selectivity between normal and cancer cells usually leaded to serious adverse effects including the gastrointestinal tract (e.g., vomiting and diarrhea) and a severe impact on the bone marrow (e.g., neutropenia), and then becoming the obstacle in clinical drug application [12-14]. Thus, the high rate of irinotecan toxicity has encouraged the development of the effective treatment method to reduce the drug's severe side effects.

Several approaches, such as the development of pro-drugs (e.g., conjugates and polymer bound irinotecan), different carrier types (e.g., liposomes, polymeric nanoparticles, and inorganic materials), have been employed with some success for irinotecan delivery [15-19]. Study has demonstrated that most of polymeric nanoparticles showed promising *in vitro* and *in vivo* results, while most of the nanocarriers did not possess therapeutic efficacy by themselves and the limited capacity to load drugs [21-23]. More importantly, some nanocarriers might cause side effects, such as toxicity and inflammation toward to organs (e.g., kidneys and liver) in the process of metabolism. Recently, some studies suggested that introduction of phosphate ester or bisphosphonate ester moiety to anticancer agents (e.g., cisplatin, camptothecin and doxorubicin) could effectively improve the antitumor activity and the solubility of drugs [23-25]. Moreover,

owing to alkaline phosphatase high-expressed in the extracellular space of cancer cells such as hepatic carcinoma and ovarian tumor cells, indicating introduction of phosphate esters group in anticancer drugs is a promising strategy to develop targeted anticancer agents [26]. In addition, phosphates or bisphosphonates have high affinity to calcium ions and display significant inhibition to osteoclastic resorption or anticancer effects in preclinical models [23, 27-29]. Some phosphate esters have been applied to design targeted drugs for bone cancer due to their high affinity to calcium ions [28, 29]. Thus, the incorporation of aminophosphonate esters group with chemotherapy drugs could potentially obtain anticancer agents with bone-targeting ability. More importantly, most natural or synthetic aminophosphonate compounds have been found to show moderate cytotoxic activity against a variety of human cancer cell lines, which can inhibit enzymes of different class and origin (e.g., matrix metalloproteinases) [29-34]. Therefore, the introduction of aminophosphonate esters group to anticancer drug irinotecan (Ir) is expected to target tumor tissue and increase the antitumor activity of Ir.

Given these considerations, we postulated that the introduction of an aminophosphonate ester group at the anticancer drug irinotecan could lead to enhance efficacy and reduce side effects as well as optimize the physicochemical properties of a new irinotecan-related anticancer drug candidate. Here, in the present study, we introduced the functional fragment aminophosphonate ester groups into irinotecan at the C-20 position via esterification reaction, and synthesized a new series of derivatives of irinotecan as potential anticancer agents.

2. **Results and discussion**

2.1. Synthesis and characterization

The synthetic route of the target irinotecan derivatives is shown in **Scheme** 1. The aminophosphonate ester moieties (**5** and **6**) were synthesized according to the reported procedures [25, 35]. Firstly, compounds **3** and **4** were prepared by the treatment of 2-(4-aminophenyl)acetic acid or 4-(4-aminophenyl)butyric acid with aromatic aldehydes (**1**) in methanol. Secondly, the intermediate compounds **5** and **6** were then obtained in good yields by addition reaction of **3** and **4** treated with diethyl phosphate, respectively. Finally, the target irinotecan derivatives **8-9** were prepared by the treatment of compounds **5** and **6** with DCC, DMAP, and irinotecan in dichloromethane at 30□ for overnight. Moreover, all target compounds (**8-9**) were characterized by ^{1}H and ^{13}C NMR spectra as well as high resolution mass spectroscopy (HR-MS). The purity of all target compounds (**8** and **9**) were ≥95% as determined by HPLC with a Symmetry C18 column (4.6 × 250 mm, 5 μm) and the spectral data in the experimental section.

2.2. In vitro cytotoxicity.

The twenty novel irinotecan (Ir)-derivatives **8a-8j** and **9a-9j** were evaluated for *in vitro* anti-proliferative activity against five human cancer cells including A549 (lung), MCF-7 (breast), MG-63 (osteosarcoma), SK-OV-3 (ovarian) and SK-OV-3/CDDP (cisplatin resistance cells) using MTT assay with triplicate experiments. Ir and CDDP were served as positive drugs, and the screening results are shown in Table 1. From the results of the MTT assay, all twenty new target compounds (**8a-8j** and **9a-9j**) showed efficient i*n vitro* cytotoxic activity against the tested five human tumor cell lines, with IC_{50} values ranging from 0.92 to 16.08 μM, indicating that both the R_1 and R_2 groups into the benzene ring might influence the cytotoxic activity of the new Ir-derivatives. As shown in table 1, most of synthesized new compounds (e.g., **8b**, **8f**, **8g**, **9b**, **9e**, **9f**, **9g** and **9j**) exhibited superior cytotoxic activity compared to the positive drug cisplatin against the five human cancer cell lines, and all compounds displayed better antitumor activities against SK-OV-3/CDDP cells than that of cisplatin, respectively. Moreover, all of the new compounds (except **8h**, **8i** and **9h**) equivalent or superior antitumor activities compared to the reference drug Ir against the tested human cancer cells. Especially, among the newly synthesized title compounds, **9b** was the most potent compound against the five tested human cancer cells, with IC_{50} values ranging from 0.92 to 4.20 μM, respectively. Notably, **9b** also showed greater anticancer activity against SK-OV-3/CDPP cells (IC_{50} = 1.39±1.02 μM) compared with the reference drugs Ir (IC_{50} = 26.55±2.33) and cisplatin (37.45±1.09 μM), respectively. Interestingly, it was noted that all target compounds (except for **8c** and **9b**) displayed better antitumor activities against two human osteosarcoma cells MG-63 and U2OS than those compounds toward other human cancer cells such as A549 (lung), MCF-7 (breast), SK-OV-3 (ovarian) an SK-OV-3/CDDP cells, indicating these irinotecan (Ir)-derivatives have a selective toxicity for the MG-63 and U2OS cells. Therefore, these results seemed to indicate that introduction of functional fragment aminophosphonate ester in Ir could potentially obtain anticancer agents with bone-targeting ability.

Structure-activity relationship (SAR) correlations were also identified for the synthesized new compounds. As shown in Table 1, compounds **8h** and **8i**, which contain –Cl and -Br (R_1) into the para-position of the benzene ring, displayed relatively lower antiproliferative activity against four human cancer cells including A549, MCF-7, SK-OV-3 and SK-OV-3/CDDP cell lines. In contrast, moving the –Cl group from the meta-position to the para-position (R_2) significantly increased the

anti-proliferative activity. The similar results were also observed in compounds **9a-9j**. Moreover, when the group was fixed as $–OCH_3$, -F, into the benzene ring of para-position (R_2) or meta-position (R_1), such as compounds **8b**, **8c**, **8e**, **8g**, **8j** and **9b**, **9c**, **9e**, **9g** and **9j**, caused a significant increase in anti-proliferative efficacy compared to **8a** and **9a**. More importantly, the similar results were also observed in compounds **9a-9j**. Moreover, compounds **8a-8j** and **9a-9j**, had different in the carbon chain length, exhibited different cytotoxic activity toward to human cancer cells. As shown in Table 1, target compounds **9a-9j** exhibited better anticancer activities against five human cancer cells than that of compounds **8a-8j**, indicating increase of the carbon chain length could increase the antitumor activity of the compound. Taken together, these findings suggested that introduction of electron-donating group (such as $-OCH_3$ group) or strong electron withdrawing groups (such as -F group) into the benzene ring of para-position or meta-position, and then an increase of the carbon chain length, might be obtained the best results.

*2.3. HPLC Analyses on the stability of compound **9b**.*

The stability of compound **9b** dissolved in PBS (pH 7.4) with or without 10% FBS examined by HPLC technique at different time, and the corresponding chromatograms were shown in **Fig. S1**. As shown in **Fig. S1**, it was observed that **9b** kept unchangeable in a period of 24 h, indicating that the designed compound **9b** was stable under the tested conditions.

*2.4. Antitumor effect of compound **9b** in vivo.*

Compound **9b** was chosen to investigate the *in vivo* anticancer efficacy owing to its excellent antitumor activity against the tested human cancer cell lines. SK-OV-3 tumor-bearing BALB/c nude mice were used as the animal mode and intravenously injected with free irinotecan (Ir) and compound **9b**, respectively. As shown in **Fig.2** B and D, the growth of SK-OV-3 tumor xenograft was significantly suppressed by 47.7% and 56.8% (IRT, inhibition rate of tumor growth) after treatment groups were injected with **9b** at two doses (10 and 20 (mg/kg)/7days) for three weeks in the SK-OV-3 tumor model, respectively. Interestingly, **9b** exhibited better antitumor activity (IRT = 56.8%) than the reference drug Ir (IRT = 53.5%), as evidenced by changes in the weight of the mice after intravenously injected with **9b** (20 mg/kg, equal weighting dose to Ir) over the course of treatment. More importantly, it was noted that conjugation of Ir with aminophosphonate ester species not only improved therapeutic effects, but also reduced the toxicity of Ir as evidenced by the inhibition of tumor growth (**Fig.2** B and D) and less decline of body weight than the reference

drug Ir (**Fig.2 C**). Furthermore, the toxicity was further evaluated by histological images in major organs (liver, heart, lung, kidney and spleen) through H&E staining. As shown in the **Fig.3**, H&E staining of the organs collected at the end of the study also indicated no observable major organ-related toxicities. Therefore, these results demonstrated that **9b** was efficacious in inhibiting the growth of SK-OV-3 tumor xenograft *in vivo* and deserved further evaluation.

*2.5. Anticancer mechanism of compound **9b**.*

2.5.1 Topo I inhibitory activity.

To further investigate the mechanism by which our synthetic compound **9b** inhibited Top I and thereby caused cytotoxicity, the effect of **9b** on Top I activity was detected by measuring the relaxation of supercoiled DNA of plasmid pBR322, and the Ir was served as positive drug. As shown in **Fig.4**, the supercoiled form (lower bands) increased after treatment with **9b** at the indicated concentrations, indicating the Topo I inhibitory activity of **9b**, and the positive drug Ir (100 and 150 μM) was found to inhibit Topo I activity as expected. Notably, it was noted that **9b** inhibited Topo I activity in this cell-free assay in a concentration-dependent manner, and similar to Ir (**Fig.4**). Thus, these results indicated that **9b** may be a new class of Topo I inhibitor.

2.5.2 Induction of apoptosis.

To further study the anticancer ability of compound **9b**, cell apoptosis investigation was carried out, and the SK-OV-3 cells was used the FITC-Annexin V/propidium iodide (PI) stain, with Ir as positive control. The untreated cells were used as control. As shown in **Fig.5**, the flow cytometry analysis results showed that the ratio of apoptosis cells was 12.02% (including the early and late apoptosis) induced by Ir. Notably, after treatment with 5.0 or 10 μM of **9b** for 24 h, the percentage of apoptosis cells (including the early and late apoptosis) is increased from 21.11% to 32.27%, respectively. Interestingly, the apoptosis rate of **9b** was significantly greater than that of Ir in early apoptosis under the same concentrations (6.24% vs 25.47%). In shorts, these results suggested that **9b** triggered SK-OV-3 cells death through apoptotic pathway.

2.5.3 Cell morphological evaluation.

The ability of compound **9b** to induce apoptosis was further evaluated by analyzing the cell morphology of the exposed SK-OV-3 cells. Thus, the cells were stained with Calcine AM and propidium iodide (PI) to mark living (green) and apoptotic (red) cells (including the early and late apoptosis), respectively. As shown in **Fig.6**, for the control group, vast majority of cells is alive. It

was noted that most of cells incubated with compound **9b** were killed in the group, in comparison, the cells in Ir group are only a few killed after incubation. Overall, these results further demonstrated that compound **9b** significantly induced apoptosis in SK-OV-3 cells.

*2.5.4. **9b** inhibited the migration of SK-OV-3 cells in vitro.*

The effect of **9b** on cell migration, which was a major mechanism involved in tumor invasion and migration, was also examined through scratching a SK-OV-3 cells monolayer and monitoring the percentage of wound closure. As illustrated in **Fig. 7**, the wounds of SK-OV-3 cells exhibited 56.9% closure in the absence of drug treatment after 24 h. In comparison to the control group, the wounds of cells exhibited 51.2% closure after incubation of Ir at 10 μM for 24 h (**Fig. 7**). Interestingly, the wounds of SK-OV-3 cells exhibited 48.9% and 42.8% after incubation of **9b** at 5.0 and 10 μM for 24 h compared to control cells, respectively (**Fig. 7**). In shorts, these results indicated that **9b** remarkably attenuated the migration of SK-OV-3 cells.

2.5.5 Cell cycle analysis.

We also investigated the effect of compound **9b** on cell cycle by measuring DNA content via a flow cytometry. As shown in **Fig. 8**, in comparison to the control group, the cell cycle was obviously changed after incubation with **9b** at 5.0 and 10 μM: the percentage of S stage increases to 27.86% and 41.40%, respectively. In addition, cells treated with Ir at 10 μM exhibit a similar cell cycle to that of the **9b** group cells (**Fig. 8**). In shorts, these results clearly suggested that **9b** caused arrest in the S stage in SK-OV-3 cells.

*2.5.6 **9b** triggered mitochondrial pathway dependent apoptosis.*

Several studies demonstrated that mitochondria play an important role in controlling cellular functions, and mitochondrial dysfunction usually triggered cell apoptosis [36, 37]. Here, in order to further examine whether **9b** induced SK-OV-3 cells apoptosis was involved in a disruption of mitochondrial membrane integrity, thus, the fluorescent probe JC-1 was used to detect the mitochondrial membrane potential (MMP) using flow cytometry analysis. As shown in **Fig. 9**, the MMP level in SK-OV-3 cells was decreased to 81.99% than that of control cells (97.87%) after incubation of Ir at 10 μM for 24 h. Interestingly, in comparison of control cells, the MMP level in SK-OV-3 cells was decreased to 80.86% and 61.59% after incubation of **9b** at 5.0 and 10 μM for 24 h, respectively (**Fig. 9**). These results indicated that cells incubation of **9b** triggered a decrease the MMP level in a concentration-dependent manner, which indicated the activation of

mitochondria mediated apoptosis.

*2.5.7 **9b** triggered reactive oxygen species (ROS) generation.*

Increasing evidence demonstrated that intracellular reactive oxygen species (ROS) generation was closely connected with apoptosis [38-40]. Here, intracellular ROS level was therefore investigated by 2′, 7′-dichlorofluoresceindiacetate (DCFH-DA) in the presence or absence of **9b**. As shown in **Fig. 10**, the production of ROS level was increased to 21.58% than that of control group cells (2.63%) after incubation of Ir at 10 μM for 24 h. Interestingly, in comparison of control group cells, **9b** induced the production of ROS level in a dose-dependent manner, and the production of ROS level in SK-OV-3 cells was increased to 28.27% and 37.49%, respectively (**Fig. 10**). Notably, after cells exposure to 10 μM of **9b**, the production of ROS level was almost twice compared to positive drug Ir (21.58% vs 37.49%). All in all, these results suggested that ROS may mediate cell apoptosis in the presence of **9b**.

*2.5.8 **9b** regulates the expression of apoptosis-related proteins.*

The above results suggested that **9b** induced cell apoptosis was closely connected with mitochondrial pathway. Bcl-2 family proteins play an important role in mitochondrial stress-induced cellular apoptosis [41, 42]. Thus, the expression of apoptosis-related proteins (such as Bcl-2 and Bax) was also investigated using western blot assay. First, SK-OV-3 cells were incubated with **9b** (5.0 and 10 μM) and Ir (10 μM) for 24 h, and the untreated SK-OV-3 cells were served as negative control, and cells treated with Ir (10 μM) were used as positive control. As shown in **Fig. 11**, **9b** markedly up-regulated the expression of Bax protein (pro-apoptotic protein) and correspondingly down-regulated the expression of Bcl-2 protein (anti-apoptotic protein) in comparison of untreated control cells. Moreover, many studies indicated that caspase-3 and -9 has been regarded as an important effector of cell apoptosis and confirmed as being activated in response to anticancer agents [43, 44]. Thus, to further evaluate if the caspase-3 and -9 was activated by compound **9b**, the western blot analysis was used to evaluate the expression of caspase-3 and -9 proteins. The western blot results suggested that the expression of caspase-3 and -9 proteins were clearly increased by **9b** or Ir compared to untreated control cells (**Fig. 11**). Notably, the above results clearly suggested that although Bax, Bcl-2, caspase-3 and -9 could be activated by Ir, whereas the **9b** was the most significant one to promote the activation of these proteins.

3. Conclusion

In summary, a novel series of aminophosphonates derivatives conjugated irinotecan were designed and synthesized, and also evaluated for anti-proliferative activity by MTT assay. The *in vitro* assays revealed that all twenty new target compounds (**8a-8j** and **9a-9j**) exhibited comparable or superior cytotoxic activity compared to the reference drug irinotecan. Especially, most of the synthesized new compounds were far more potent than reference drugs irinotecan and cisplatin against SK-OV-3/CDDP cells. Moreover, the *in vitro* assay results indicated that the electron-donating group (such as -OCH_3 group) or strong electron withdrawing group (such as -F group) into the benzene ring of para-position or meta-position and then an increase of the carbon chain length (e.g., **9b**, **9c**, **9e**, **9g** and **9j**), exhibited much improved potency in comparison to other analogues in this series. Among them, **9b**, the most potent compound, exhibited a 5.4~19.1-fold increase in activity when compare with anticancer drug irinotecan, with IC_{50} values of 0.92-3.23 μM against five human cancer cells, respectively. Furthermore, **9b** significantly caused cell cycle arrest at the S stage and induced apoptosis in SK-OV-3 cells through mitochondrial-dependent apoptosis pathway. Moreover, most of target compounds (**8** and **9**) displayed better antitumor activities against two human osteosarcoma cells MG-63 and U2OS than those compounds toward to other four human cancer cells, suggesting these compounds were promisingly bone-targeting agents. More importantly, **9b** significantly inhibited tumor growth in mouse xenograft models and had no observable toxic effect. Upon the significant antitumor efficacy both *in vitro* and *in vivo*, further development of **9b**-related compounds as potential anticancer clinical trial candidates was definitely warranted. Furthermore, the pharmacokinetic profile of compound **9b** still need to be improved and its therapeutic advantages over the reference drug irinotecan remain to be further evaluated.

4. Experimental section

All chemicals and solvents were analytical reagent grade and commercially available, and used without further purification. Column chromatography was performed using silica gel (200–300 mesh). Mass spectra were measured on a Thermo Scientific LC/MS instrument. ^{1}H NMR and ^{13}C NMR spectra were recorded in $CDCl_3$ or DMSO-*d6* with a Bruker 400 or 600 MHz NMR spectrometer.

*4.1. General procedure for the preparation of compounds **8a-8j** and **9a-9j**.*

Synthesis of compounds **5a** and **6a** [25, 35]. To solution of benzaldehyde (**1**, 1.17 g, 11.0 mmol) and 4-(4-aminophenyl) acetic acid (**2**, 1.51 g, 10.0 mmol) or 4-(4-aminophenyl) butyric acid (**3**, 1.79 g, 10.0 mmol) in dry methanol (50 mL), and added some anhydrous Na_2SO_4 (284 mg, 2.0 mmol) in reaction, and then the mixture was stirred and refluxed for overnight. After completion, the solvent was removed under reduced pressure to obtain the intermediated **3** or **4**, to which was added diethyl phosphite (8 mL), and the mixture was stirred at 50 °C for 2~3 h. After completion of reaction, the reaction mixture was diluted with dichloromethane (200 mL), and washed three times with water (3 × 300 mL). The organic phase was dried over anhydrous Na_2SO_4 and concentrated under vacuum. The residue was purified on silica gel column, eluting with CH_3OH/CH_2Cl_2 = 1:100, 1:80) to obtain the desire **5a** (2.8 g, yield 70.89%) or **6a** (3.2 g, yield 76.4%) as a white solid.

Compound **5a**. ^{1}H NMR (600 MHz, DMSO-*d6*) δ 12.10 (s, 1H), 7.52 (d, *J* = 7.6 Hz, 2H), 7.31 (t, *J* = 7.6 Hz, 2H), 7.23 (t, *J* = 7.2 Hz, 1H), 6.89 (d, *J* = 8.4 Hz, 2H), 6.73 (d, *J* = 8.5 Hz, 2H), 6.30 – 6.27 (m, 1H), 5.04 – 4.98 (m, 1H), 4.08 – 4.02 (m, 2H), 3.91 – 3.87 (m, 1H), 3.73 – 3.68 (m, 1H), 3.31 (s, 2H), 1.19 (t, *J* = 7.0 Hz, 3H), 1.04 (t, *J* = 7.0 Hz, 3H). ^{13}C NMR (150 MHz, DMSO-*d6*) δ 173.70, 146.36, 146.28, 137.41, 130.02, 128.80, 128.42, 127.82, 123.56, 113.87, 62.97, 62.67, 54.94, 53.93, 16.81, 16.54.

Compound **6a**. ^{1}H NMR (400 MHz, DMSO-*d6*) δ 11.97 (s, 1H), 7.52 (d, *J* = 7.1 Hz, 2H), 7.31 (t, *J* = 7.3 Hz, 2H), 7.24 – 7.21 (m, 1H), 6.83 (d, *J* = 8.1 Hz, 2H), 6.71 (d, *J* = 8.1 Hz, 2H), 6.27 – 6.05 (m, 1H), 5.02 – 4.93 (m, 1H), 4.16 – 4.03 (m, 2H), 3.92 – 3.84 (m, 1H), 3.75 – 3.67 (m, 1H), 2.37 (t, *J* = 7.3 Hz, 2H), 2.14 (t, *J* = 7.2 Hz, 2H), 1.71– 1.64 (m, 2H), 1.18 (t, *J* = 7.0 Hz, 3H), 1.04 (t, *J* = 7.0 Hz, 3H). ^{13}C NMR (100 MHz, DMSO-*d6*) δ 174.81, 145.77, 145.62, 137.53, 130.22, 128.99, 128.83, 128.42, 127.81, 114.07, 62.95, 62.66, 55.41, 53.90, 34.01, 33.54, 27.07, 16.79, 16.53.

General synthesis of compounds **8a-8j** and **9a-9j**. To a solution of **5** or **6** (1.0 equiv), DCC (1.5 equiv), and DMAP (0.2 equiv) in dry CH_2Cl_2 (4 mL), Ir (44 mg, 0.071 mmol, 0.2 equiv) was added in portions, and the mixture was stirred at 30 □ for overnight. After completion, the reaction mixture was filtered to remove white solids (dicyclohexylurea) and the filtrate was concentrated under vacuum. Then, the residue was purified on silica gel column, eluting with a mixing solvent (CH_3OH/CH_2Cl_2 = 1:80, 1: 60, 1:40, 1:30) to obtain the desired compounds **8a-8j**

and **9a-9j** as a yellow solid. The resulting compounds were confirmed by ^{1}H NMR, ^{13}C NMR, and HR-MS spectra.

Compound **8a**. 45 mg, yield: 67.2%. ^{1}H NMR (600 MHz, $CDCl_3$) δ 8.26 – 8.23 (m, 1H), 7.87 (d, *J* = 2.2 Hz, 1H), 7.65 – 7.62 (m, 1H), 7.41 (t, *J* = 7.8 Hz, 2H), 7.28 – 7.22 (m, 3H), 7.12 (d, *J* = 3.7 Hz, 1H), 7.02– 6.99 (m, 2H), 6.55– 6.52 (m, 2H), 5.63 (d, *J* = 17.2 Hz, 1H), 5.39 (d, *J* = 17.2 Hz, 1H), 5.23 (d, *J* = 4.2 Hz, 2H), 4.82– 4.66 (m, 2H), 4.52– 4.40 (m, 2H), 4.12 – 4.05 (m, 2H), 3.94 – 3.89 (m, 1H), 3.70 – 3.61 (m, 3H), 3.19– 3.07 (m, 3H), 2.96 – 2.77 (m, 5H), 2.31 – 2.24 (m, 1H), 2.17 – 2.07 (m, 3H), 1.88 – 1.69 (m, 6H), 1.55 (s, 2H), 1.41 (t, *J* = 7.7 Hz, 3H), 1.26 (t, *J* = 7.3 Hz, 3H), 1.11 – 1.07 (m, 3H), 0.94 – 0.91 (m, 3H). ^{13}C NMR (150 MHz, $CDCl_3$) δ 171.23, 167.52, 157.32, 153.05, 151.52, 150.30, 147.14, 146.75, 145.70, 145.46, 145.32, 135.67, 131.66, 130.18, 128.55, 127.92, 127.81, 127.78, 127.52, 127.08, 125.94, 122.39, 120.12, 114.65, 114.04, 95.89, 75.99, 67.14, 63.34, 63.30, 63.23, 62.70, 56.47, 55.47, 50.17, 49.24, 44.10, 43.75, 39.53, 31.84, 29.70, 27.71, 26.96, 25.13, 23.93, 23.18, 16.75, 16.43, 16.19, 14.04, 7.52. HR-MS (m/z) (ESI): calcd for $C_{52}H_{60}N_5O_{10}P$ $[M+H]^+$: 946.4156; found: 946.4123. Purity: 98.00% (by HPLC), t_R = 17.897 min.

Compound **8b**. 50 mg, yield: 73.5%. ^{1}H NMR (600 MHz, $CDCl_3$) δ 8.21 (d, *J* = 9.2 Hz, 1H), 7.84 (d, *J* = 2.3 Hz, 1H), 7.60 (d, *J* = 9.2 Hz, 1H), 7.38 – 7.32 (m, 2H), 7.09 (d, *J* = 2.4 Hz, 1H), 7.00 – 6.92 (m, 2H), 6.94 (t, *J* = 8.5 Hz, 2H), 6.50 – 6.47 (m, 2H), 5.60 (d, *J* = 17.2 Hz, 1H), 5.37 (d, *J* = 17.2 Hz, 1H), 5.20 (d, *J* = 4.6 Hz, 2H), 4.74 – 4.60 (m, 2H), 4.48 – 4.36 (m, 2H), 4.11 – 4.00 (m, 2H), 3.95 – 3.88 (m, 1H), 3.73 – 3.67 (m, 1H), 3.64 – 3.59 (m, 2H), 3.16 – 3.07 (m, 3H), 2.93 – 2.71 (m, 6H), 2.30 – 2.21 (m, 1H), 2.14 – 2.01 (m, 3H), 1.83 – 1.60 (s, 6H), 1.57 – 1.46 (s, 2H), 1.38 (t, *J* = 7.7 Hz, 3H), 1.24 (d, *J* = 6.6 Hz, 3H), 1.12 – 1.08 (m, 3H), 0.93 – 0.88 (m, 3H). ^{13}C NMR (150 MHz, $CDCl_3$) δ 171.20, 167.52, 163.19, 161.54, 157.33, 153.06, 151.51, 150.33, 147.12, 146.74, 145.70, 145.36, 145.26, 145.16, 131.61, 131.46, 130.23, 129.40, 129.35, 129.32, 127.53, 127.09, 125.96, 122.64, 120.10, 115.58, 115.45, 114.65, 114.04, 95.88, 76.03, 67.14, 63.42, 63.33, 63.29, 62.57, 55.78, 54.78, 50.14, 49.25, 44.17, 43.82, 39.53, 31.83, 29.70, 27.79, 27.04, 25.31, 24.06, 23.18, 16.43, 16.23, 14.03, 7.52. HR-MS (m/z) (ESI): calcd for $C_{52}H_{59}FN_5O_{10}P$ $[M+H]^+$: 964.4062; found: 964.4023. Purity: 96.05% (by HPLC), t_R = 9.657 min.

Compound **8c**. 49 mg, yield: 70.5%. ^{1}H NMR (600 MHz, $CDCl_3$) δ 8.21 (d, *J* = 9.2 Hz, 1H), 7.84 (d, *J* = 2.4 Hz, 1H), 7.60 (d, *J* = 9.2 Hz, 1H), 7.34 – 7.29 (m, 2H), 7.22 – 7.18 (m, 2H), 7.09

(d, *J* = 4.1 Hz, 1H), 7.01 – 6.97 (m, 2H), 6.49 – 6.46 (m, 2H), 5.60 (d, *J* = 17.2 Hz, 1H), 5.37 (d, *J* = 17.2 Hz, 1H), 5.20 (d, *J* = 4.1 Hz, 2H), 4.70 – 4.70 (m, 1H), 4.68 – 4.60 (m, 1H), 4.52 – 4.41 (m, 2H), 4.10 – 4.03 (m, 2H), 3.97 – 3.91 (m, 1H), 3.73 (d, *J* = 8.5 Hz, 1H), 3.62 – 3.59 (t, *J* = 11.4 Hz, 2H), 3.17 – 3.11 (m, 3H), 2.99 – 2.88 (m, 5H), 2.30 – 2.22 (m, 2H), 2.15 – 2.08 (m, 2H), 1.90 – 1.78 (m, 6H), 1.62 – 1.54 (m, 2H), 1.38 (t, *J* = 7.6 Hz, 3H), 1.27 – 1.21 (m, 3H), 1.13 – 1.09 (m, 3H), 0.93 – 0.88 (m, 3H). ^{13}C NMR (150 MHz, $CDCl_3$) δ 171.18, 167.51, 157.32, 152.98, 151.58, 150.19, 147.16, 146.73, 145.70, 145.38, 145.19, 145.09, 134.40, 133.65, 131.66, 130.25, 129.10, 128.74, 127.51, 127.13, 125.87, 122.72, 120.12, 114.71, 114.06, 95.88, 79.04, 76.04, 67.14, 63.47, 63.39, 63.35, 62.97, 55.94, 54.94, 50.05, 49.25, 43.47, 39.55, 33.17, 31.82, 29.70, 27.21, 26.40, 24.22, 23.20, 22.70, 16.44, 16.25, 14.05, 7.53. HR-MS (m/z) (ESI): calcd for $C_{52}H_{59}ClN_5O_{10}P$ $[M+H]^+$: 980.3766; found: 980.3738. Purity: 97.28% (by HPLC), t_R = 7.396 min.

Compound **8d**. 56 mg, yield: 76.7%. ^{1}H NMR (600 MHz, $CDCl_3$) δ 8.53 (d, *J* = 9.1 Hz, 1H), 8.16 (s, 1H), 7.91 (t, *J* = 15.9 Hz, 1H), 7.69 – 7.67 (m, 2H), 7.60 – 7.55 (m, 2H), 7.41 (d, *J* = 8.3 Hz, 1H), 7.31 (t, *J* = 8.5 Hz, 2H), 6.82 – 6.79 (m, 2H), 5.93 (d, *J* = 17.0 Hz, 1H), 5.69 (d, *J* = 16.9 Hz, 1H), 5.51 (d, *J* = 6.6 Hz, 2H), 5.10 – 5.08 (m, 1H), 5.00 – 4.93 (m, 1H), 4.86 – 4.77 (m, 2H), 4.43 – 4.33 (m, 2H), 4.28 – 4.21 (m, 1H), 4.08 – 4.00 (m, 1H), 3.98– 3.93 (m, 2H), 3.66– 3.54 (s, 1H), 3.46 – 3.43 (m, 5H), 3.29 – 3.25 (m, 2H), 2.76 (d, *J* = 7.3 Hz, 1H), 2.60 – 2.54 (m, 2H), 2.45 – 2.41 (m, 5H), 2.28 – 2.18 (m, 2H), 1.97 (s, 2H), 1.69 (t, *J* = 7.2 Hz, 3H), 1.57 – 1.54 (m, 3H), 1.46 – 1.41 (m, 3H), 1.23 (t, *J* = 9.3 Hz, 3H).^{13}C NMR (150 MHz, $CDCl_3$) δ 171.17, 167.51, 157.31, 152.89, 151.62, 150.07, 147.17, 146.75, 145.73, 145.40, 145.21, 145.12, 135.00, 131.66, 130.24, 129.46, 127.49, 127.16, 125.76, 122.74, 121.82, 120.02, 114.75, 114.07, 95.85, 76.05, 67.10, 63.46, 63.40, 63.36, 56.01, 55.02, 53.50, 50.05, 49.25, 43.44, 43.05, 39.52, 31.77, 29.68, 26.61, 25.78, 23.18, 23.07, 22.60, 16.43, 16.25, 14.05, 7.53. HR-MS (m/z) (ESI): calcd for $C_{52}H_{59}BrN_5O_{10}P$ $[M+H]^+$: 1024.3261; found: 1024.3236. Purity: 99.09% (by HPLC), t_R = 7.386 min.

Compound **8e**. 44 mg, yield: 63.8%. ^{1}H NMR (600 MHz, $CDCl_3$) δ 8.22 (d, *J* = 13.0 Hz, 1H), 7.84 (s, 1H), 7.58 (d, *J* = 9.0 Hz, 1H), 7.30 – 7.28 (m, 2H), 7.08 (d, *J* = 5.8 Hz, 1H), 6.99 – 6.96 (m, 2H), 6.78 (d, *J* = 7.8 Hz, 2H), 6.51 – 6.49 (m, 2H), 5.60 (d, *J* = 17.2 Hz, 1H), 5.36 (d, *J* = 17.2 Hz, 1H), 5.19 (d, *J* = 2.6 Hz, 2H), 4.74 – 4.61 (m, 2H), 4.58 – 4.45 (m, 2H), 4.10 – 4.00 (m, 2H), 3.92 – 3.85 (m, 1H), 3.72 (s, 3H), 3.65 – 3.58 (m, 3H), 3.21 – 2.92 (m, 8H), 2.43 (d, *J* = 9.4 Hz,

1H), 2.29 – 2.22 (m, 2H), 2.13 – 2.08 (m, 5H), 1.95 – 1.80 (m, 2H), 1.71 – 1.57 (m, 2H), 1.37 (t, *J* = 7.6 Hz, 3H), 1.24 – 1.20 (m, 3H), 1.11 – 1.06 (m, 3H), 0.93 – 0.88 (m, 3H). ^{13}C NMR (150 MHz, $CDCl_3$) δ 171.25, 167.52, 159.23, 157.31, 152.90, 151.62, 150.04, 147.17, 146.72, 145.76, 145.53, 145.40, 131.75, 130.15, 128.94, 128.90, 127.48, 127.13, 125.77, 122.32, 120.09, 114.75, 114.03, 95.92, 76.01, 67.11, 63.44, 63.32, 63.27, 55.76, 55.23, 54.75, 50.02, 49.25, 43.45, 43.06, 39.55, 31.80, 29.69, 26.62, 25.76, 23.18, 23.09, 22.65, 16.45, 16.26, 14.06, 7.53. HR-MS (m/z) (ESI): calcd for $C_{53}H_{62}N_5O_{11}P$ $[M+H]^+$: 976.4262; found: 976.4224. Purity: 98.49% (by HPLC), t_R = 9.233 min.

Compound **8f**. 39 mg, yield: 57.4%. ^{1}H NMR (600 MHz, $CDCl_3$) δ 8.21 (d, *J* = 9.1 Hz, 1H), 7.83 (d, *J* = 2.4 Hz, 1H), 7.60 (d, *J* = 9.1 Hz, 1H), 7.30 – 7.23 (m, 2H), 7.10 (d, *J* = 5.8 Hz, 1H), 7.06 – 7.04 (m, 2H), 6.98 – 6.95 (m, 2H), 6.51 – 6.49 (m, 2H), 5.60 (d, *J* = 17.0 Hz, 1H), 5.37 (d, *J* = 17.2 Hz, 1H), 5.20 (d, *J* = 8.9 Hz, 2H), 4.76 – 4.73 (m, 1H), 4.68 – 4.61 (m, 1H), 4.47 (d, *J* = 12.6 Hz, 1H), 4.37 (d, *J* = 12.5 Hz, 1H), 4.11 – 4.00 (m, 2H), 3.93 – 3.85(m, 1H), 3.67 – 3.58 (m, 3H), 3.15 – 3.11 (m, 1H), 3.09 – 3.05 (m, 1H), 2.92 – 2.86 (m, 1H), 2.81 – 2.59 (m, 5H), 2.29 – 2.27 (m, 1H), 2.25 (s, 3H), 2.14 – 2.10 (m, 2H), 2.02 (d, *J* = 9.7 Hz, 1H), 1.74 – 1.62 (m, 6H), 1.56 – 1.46 (m, 2H), 1.37 (t, *J* = 7.6 Hz, 3H), 1.24 – 1.2 (m, 3H), 1.09 – 1.06 (m, 3H), 0.92 – 0.88 (m, 3H). ^{13}C NMR (150 MHz, $CDCl_3$) δ 171.24, 167.52, 157.33, 153.07, 150.34, 147.14, 146.74, 145.68, 145.52, 145.30, 137.59, 132.48, 131.66, 130.15, 129.29, 127.66, 127.52, 127.08, 125.96, 122.31, 120.14, 114.63, 114.07, 95.91, 75.98, 67.15, 63.30, 63.25, 63.22, 62.59, 56.17, 55.16, 50.18, 49.25, 44.19, 43.85, 39.54, 31.85, 29.70, 27.84, 27.10, 25.38, 24.11, 23.18, 16.45, 16.23, 14.04 (s), 7.52 (s). HR-MS (m/z) (ESI): calcd for $C_{53}H_{62}N_5O_{10}P$ $[M+H]^+$: 960.4313; found: 960.4284. Purity: 98.53% (by HPLC), t_R = 9.220 min.

Compound **8g**. 41 mg, yield: 60.3%. ^{1}H NMR (400 MHz, $CDCl_3$) δ 8.20 (d, *J* = 9.2 Hz, 1H), 7.83 (d, *J* = 1.9 Hz, 1H), 7.57 (d, *J* = 8.7 Hz, 1H), 7.22 – 7.14 (m, ,2H), 7.12 – 7.05 (m, 2H), 7.00 – 6.97 (m, 2H), 6.91 – 6.85 (m, 1H), 6.49 (d, *J* = 6.9 Hz, 2H), 5.59 (d, *J* = 17.1 Hz, 1H), 5.35 (d, *J* = 17.2 Hz, 1H), 5.18 (d, *J* = 2.4 Hz, 2H), 4.79 – 4.75 (m, 1H), 4.71 – 4.61 (m, 1H), 4.54 – 4.45 (m, 2H), 4.10 – 4.01 (m, 2H), 3.96 – 3.88 (m, 1H), 3.75 – 3.68 (m, 1H), 3.67 – 3.59 (m, 2H), 3.29 – 3.23 (m, 1H), 3.14 – 3.09 (m, 5H), 2.95 – 2.90 (m, 2H), 2.45 (d, *J* = 8.8 Hz, 1H), 2.28 – 2.21 (m, 2H), 2.13 – 1.86 (m, 7H), 1.75 – 1.54 (m, 2H), 1.36 (t, *J* = 7.6 Hz, 3H), 1.23 – 1.20 (m, 3H), 1.11 – 1.07 (m, 3H), 0.92 – 0.87 (m, 3H). ^{13}C NMR (150 MHz, $CDCl_3$) δ 171.22, 167.52, 163.68,

162.07, 157.31, 152.89, 151.60, 150.02, 147.15, 146.73, 145.75, 145.42, 145.24, 145.14, 138.66, 131.69, 130.24, 130.09, 127.48, 127.14, 125.76, 123.50, 122.68, 120.02, 114.99, 114.77, 114.59, 113.99, 95.91, 76.05, 67.10, 63.51, 63.44, 63.40, 56.15, 55.12, 50.03, 49.26, 43.39, 43.00, 39.54, 31.78, 29.69, 26.53, 25.66, 23.17, 22.93, 22.53, 16.41, 16.20, 14.05, 7.53. HR-MS (m/z) (ESI): calcd for $C_{52}H_{59}FN_5O_{10}P$ $[M+H]^+$: 964.4062; found: 964.4030. Purity: 98.56% (by HPLC), t_R = 8.000 min.

Compound **8h**. 47 mg, yield: 69.5%. ^{1}H NMR (400 MHz, $CDCl_3$) δ 8.20 (d, *J* = 9.2 Hz, 1H), 7.83 (d, *J* = 2.1 Hz, 1H), 7.57 (d, *J* = 8.9 Hz, 1H), 7.33 – 7.28 (m, *J* = 16.5, 5.3 Hz, 2H), 7.21 – 7.18 (m, 2H), 7.07 (d, *J* = 4.5 Hz, 1H), 7.00 – 6.96 (m, 2H), 6.49 – 6.46 (m, 2H), 5.59 (d, *J* = 17.1 Hz, 1H), 5.35 (d, *J* = 17.2 Hz, 1H), 5.18 (d, *J* = 2.8 Hz, 2H), 4.76 – 4.72 (m, 1H), 4.69 – 4.59 (m, 1H), 4.54 – 4.44 (m, 2H), 4.08 – 4.00 (m, 2H), 3.96 – 3.87 (m, 1H), 3.77 – 3.69 (m, 1H), 3.64 – 3.59 (m, 2H), 3.25 – 3.20 (m, 1H), 3.13 – 3.09 (m, 5H), 2.96 – 2.86 (m, 2H), 2.43 (d, *J* = 7.6 Hz, 1H), 2.28 – 2.19 (m, 2H), 2.14 – 2.07 (m, 7H), 1.72 – 1.53 (m, 2H), 1.36 (t, *J* = 7.4 Hz, 3H), 1.24 – 1.20 (m, 3H), 1.12– 1.08 (m, 3H), 0.91 – 0.85 (m, 3H). ^{13}C NMR (150 MHz, $CDCl_3$) δ 171.19, 167.50, 157.31, 152.89, 151.61, 150.04, 147.16, 146.71, 145.75, 145.42, 145.21, 145.11, 134.40, 133.63, 131.70, 130.24, 129.11, 128.73, 127.49, 127.14, 125.76, 122.70, 120.03, 114.76, 114.05, 95.89, 76.05, 67.10, 63.46, 63.40, 63.36, 55.92, 54.92, 50.03, 49.25, 43.33, 43.05, 39.55, 31.78, 29.69, 26.60, 25.75, 23.18, 23.05, 22.62, 16.43, 16.25, 14.06, 7.53. HR-MS (m/z) (ESI): calcd for $C_{52}H_{59}ClN_5O_{10}P$ $[M+H]^+$: 980.3766; found: 980.3740. Purity: 96.91% (by HPLC), t_R = 8.832 min.

Compound **8i**. 52 mg, yield: 74.3%. ^{1}H NMR (400 MHz, $CDCl_3$) δ 8.21 (d, *J* = 9.2 Hz, 1H), 7.84 (d, *J* = 2.4 Hz, 1H), 7.62 – 7.57 (m, 1H), 7.56 – 7.50 (m, 1H), 7.41 – 7.30 (m, 2H), 7.19 – 7.09 (m, 2H), 7.02 – 6.98 (m, 2H), 6.50 – 6.47 (m, 2H), 5.61 (d, *J* = 17.2 Hz, 1H), 5.37 (d, *J* = 17.2 Hz, 1H), 5.20 (d, *J* = 4.2 Hz, 2H), 4.77 – 4.71 (m, 1H), 4.68 – 4.60 (m, 1H), 4.48 (d, *J* = 12.4 Hz, 1H), 4.39 (d, *J* = 12.9 Hz, 1H), 4.12 – 4.03 (m, 2H), 3.97 – 3.90 (m, 1H), 3.76 – 3.60 (m, 3H), 3.15 – 3.05 (m, 3H), 2.94 – 2.74 (m, 5H), 2.30 – 2.20 (m, 1H), 2.14 – 2.01 (m, 3H), 1.93 – 1.78 (m, 6H), 1.65 – 1.53 (m, 2H), 1.38 (t, *J* = 7.7 Hz, 3H), 1.27 – 1.22 (m, 3H), 1.13 – 1.09 (m, 3H), 0.93 – 0.89 (m, 3H). ^{13}C NMR (150 MHz, $CDCl_3$) δ 171.19, 167.50, 157.33, 153.05, 151.53, 150.31, 147.14, 146.75, 145.70, 145.33, 145.15, 145.10, 138.41, 131.60, 131.07, 130.73, 130.28, 130.14, 127.53, 127.08, 126.35, 125.95, 122.76, 122.66, 120.13, 114.66, 113.99, 95.89, 76.03, 67.15, 63.52, 63.48, 63.43, 62.70, 56.10, 55.11, 50.19, 49.25, 44.12, 43.77, 39.52, 31.84, 29.70, 27.74,

26.98, 25.17, 23.97, 23.19, 16.42, 16.20, 14.04, 7.53. HR-MS (m/z) (ESI): calcd for $C_{52}H_{59}BrN_5O_{10}P$ $[M+H]^+$: 1024.3261; found: 1024.3223. Purity: 96.08% (by HPLC), t_R = 9.972 min.

Compound **8j**. 40 mg, yield: 57.8%. ^{1}H NMR (400 MHz, $CDCl_3$) δ 8.24 (d, *J* = 9.2 Hz, 1H), 7.85 (d, *J* = 2.1 Hz, 1H), 7.64 – 7.61 (m, 1H), 7.18 (t, *J* = 7.8 Hz, 1H), 7.11 (d, *J* = 3.1 Hz, 1H), 7.01 – 6.96 (m, 4H), 6.82 – 6.74 (m, 1H), 6.54 – 6.52 (m, 2H), 5.62 (d, *J* = 17.2 Hz, 1H), 5.38 (d, *J* = 17.2 Hz, 1H), 5.22 (d, *J* = 3.4 Hz, 2H), 4.79 – 4.75 (m, 1H), 4.71 – 4.62 (m, 1H), 4.49 (d, *J* = 12.5 Hz, 1H), 4.40 (d, *J* = 12.0 Hz, 1H), 4.13 – 4.04 (m, 2H), 3.94 – 3.89 (m, 1H), 3.74 (s, 3H), 3.71 – 3.60 (m, 3H), 3.18 – 3.06 (m, 3H), 2.95 – 2.76 (m, 5H), 2.30 – 2.24 (m, 1H), 2.16 – 2.05 (m, 3H), 1.92 – 1.70 (m, 6H), 1.60 – 1.48 (m, 2H), 1.39 (t, *J* = 7.5 Hz, 3H), 1.29 – 1.23 (m, 3H), 1.12 – 1.08 (m, 3H), 0.95 – 0.91 (m, 3H). ^{13}C NMR (150 MHz, $CDCl_3$) δ 171.24, 167.53, 159.73, 157.33, 153.05, 151.52, 150.30, 147.13, 146.75, 145.73, 145.51, 145.42, 145.33, 131.66, 130.18, 129.54, 127.52, 127.09, 125.94, 122.42, 120.18, 114.64, 114.03, 113.49, 113.31, 95.90, 76.00, 67.14, 63.40, 63.33, 63.29, 56.53, 55.53, 55.21, 50.18, 49.25, 44.09, 43.74, 39.53, 31.83, 29.70, 27.70, 26.95, 25.11, 23.92, 23.18, 16.44, 16.22, 14.04, 7.52. HR-MS (m/z) (ESI): calcd for $C_{53}H_{62}N_5O_{11}P$ $[M+H]^+$:976.4262; found: 976.4249. Purity: 95.98% (by HPLC), t_R = 9.993 min.

Compound **9a**. 46 mg, yield: 66.7%. ^{1}H NMR (600 MHz, $CDCl_3$) δ 8.16 (d, *J* = 8.8 Hz, 1H), 7.82 (d, *J* = 1.9 Hz, 1H), 7.58 – 7.56 (m, 1H), 7.43 (d, *J* = 7.1 Hz, 2H), 7.30 – 7.28 (m, 2H), 7.24 – 7.20 (m, 1H), 7.14 (s, 1H), 6.90 (d, *J* = 8.2 Hz, 2H), 6.49 (d, *J* = 8.2 Hz, 2H), 5.65 (d, *J* = 17.0 Hz, 1H), 5.39 (d, *J* = 17.0 Hz, 1H), 5.22 (d, *J* = 4.6 Hz, 2H), 4.74 – 4.68 (m, 2H), 4.48 (d, *J* = 12.7 Hz, 1H), 4.38 (d, *J* = 12.7 Hz, 1H), 4.12 – 4.04 (m, 2H), 3.94 – 3.88 (m, 1H), 3.68 – 3.63 (m, 1H), 3.15 – 3.05 (m, 3H), 2.92 – 2.74 (m, 5H), 2.48 (t, *J* = 10.3 Hz, 2H), 2.45 – 2.36 (m, 2H), 2.26 – 2.19 (m, 1H), 2.12 – 2.04 (m, 3H), 1.87 – 1.82 (m, 2H), 1.78 – 1.68 (m, 6H), 1.57 – 1.47 (m, 2H), 1.37 (t, *J* = 7.7 Hz, 3H), 1.26 – 1.24 (m, 3H), 1.09 (t, *J* = 7.0 Hz, 3H), 0.93 (t, *J* = 7.4 Hz, 3H). ^{13}C NMR (150 MHz, $CDCl_3$) δ 172.56, 167.64, 157.38, 153.04, 151.51, 150.29, 147.12, 146.75, 146.03, 145.37, 144.51, 144.41, 135.92, 131.59, 131.00, 129.23, 128.58, 127.85, 127.53, 127.11, 125.88, 120.01, 114.63, 113.95, 95.91, 75.69, 67.10, 63.33, 63.30, 63.25, 62.66, 56.69, 55.69, 50.12, 49.28, 44.11, 43.75, 33.84, 32.97, 31.81, 29.70, 27.67, 26.91, 26.34, 25.07, 23.92, 23.18, 16.46, 16.22, 14.03, 7.59. HR-MS (m/z) (ESI): calcd for $C_{54}H_{64}N_5O_{10}P$ $[M+H]^+$: 974.4469; found: 974.4432. Purity: 97.87% (by HPLC), t_R = 10.167 min.

Compound **9b**. 51 mg, yield: 72.8%. ^{1}H NMR (400 MHz, CD_2Cl_2) δ 8.16 (d, *J* = 9.0 Hz, 1H), 7.83 (d, *J* = 1.1 Hz, 1H), 7.57 (d, *J* = 8.7 Hz, 1H), 7.49 – 7.36 (m, 2H), 7.14 (s, 1H), 7.02 – 6.99 (m, 2H), 6.91 (d, *J* = 7.6 Hz, 2H), 6.47 (d, *J* = 7.9 Hz, 2H), 5.65 (d, *J* = 17.2 Hz, 1H), 5.39 (d, *J* = 17.2 Hz, 1H), 5.25 (d, *J* = 4.6 Hz, 2H), 4.78 – 4.69 (m, 2H), 4.48 (d, *J* = 12.6 Hz, 1H), 4.40 (d, *J* = 12.0 Hz, 1H), 4.14 – 4.03 (m, 2H), 3.98 – 3.91 (m, 1H), 3.76 – 3.70 (m, 1H), 3.16 – 3.05 (m, 3H), 2.93 – 2.79 (m, 5H), 2.50 (t, *J* = 7.3 Hz, 2H), 2.45 – 2.34 (m, 2H), 2.29 – 2.22 (m, 1H), 2.17– 2.07 (m, 3H), 1.94 – 1.73 (m, 8H), 1.60 – 1.48 (m, 2H), 1.37 (t, *J* = 7.4 Hz, 3H), 1.27 – 1.24 (m, 3H), 1.12 (t, *J* = 7.0 Hz, 3H), 0.94 (t, *J* = 7.3 Hz, 3H). ^{13}C NMR (150 MHz, $CDCl_3$) δ 172.54, 167.64, 163.21, 161.57, 157.37, 153.01, 151.54, 150.25, 147.14, 146.74, 146.02, 145.39, 144.30, 144.20, 131.72, 131.58, 131.21, 129.42, 129.28, 129.23, 127.54, 127.12, 125.85, 120.02, 115.63, 115.48, 114.64, 113.94, 95.89, 75.71, 67.10, 63.43, 63.29, 62.68, 56.00, 55.03, 49.99, 49.28, 44.40, 43.65, 34.48, 33.82, 32.95, 31.81, 29.70, 27.43, 26.64, 26.34, 24.67, 23.71, 23.19, 16.47, 16.27, 14.04, 7.59. HR-MS (m/z) (ESI): calcd for $C_{54}H_{63}FN_5O_{10}P$ $[M+H]^+$: 992.4375; found: 992.4346. Purity: 96.05% (by HPLC), t_R = 8.855 min.

Compound **9c**. 48 mg, yield: 67.6%. ^{1}H NMR (600 MHz, $CDCl_3$) δ 8.16 (d, *J* = 10.9 Hz, 1H), 7.87 (d, *J* = 3.4 Hz, 1H), 7.58 – 7.55 (m, 1H), 7.37 (d, *J* = 7.5 Hz, 2H), 7.31 – 7.28 (m, 2H), 7.14 (s, 1H), 7.03 – 6.81 (m, 2H), 6.91 – 6.89 (m, 2H), 5.65 (d, *J* = 17.0 Hz, 1H), 5.39 (d, *J* = 17.0 Hz, 1H), 5.21 (d, *J* = 4.7 Hz, 2H), 4.70 – 4.65 (m, 2H), 4.48 (d, *J* = 11.8 Hz, 1H), 4.39 (d, *J* = 12.1 Hz, 1H), 4.12 – 4.04 (m, 2H), 3.98 – 3.92 (m, 1H), 3.77 – 3.72 (m, 1H), 3.15 – 3.06 (m, 3H), 2.92 – 2.77 (m, 5H), 2.50 – 2.48 (m, 2H), 2.45 – 2.38 (m, 2H), 2.26 – 2.22 (m, 1H), 2.18 – 2.06 (m, 3H), 1.91 – 1.80 (m, 8H), 1.59 – 1.47 (m, 2H), 1.37 (t, *J* = 7.4 Hz, 3H), 1.26 – 1.23 (m, 3H), 1.13 (t, *J* = 7.0 Hz, 3H), 0.93 (t, *J* = 7.4 Hz, 3H). ^{13}C NMR (150 MHz, $CDCl_3$) δ 172.54, 167.65, 157.37, 153.03, 151.52, 150.27, 147.13, 146.75, 146.02, 145.39, 144.22, 144.12, 134.66, 133.63, 131.57, 131.30, 129.30, 129.16, 128.76, 127.54, 127.12, 125.87, 120.01, 114.64, 113.94, 95.89, 75.71, 67.10, 63.49, 63.33, 62.73, 56.15, 55.15, 50.13, 49.28, 43.06, 43.70, 33.81, 32.93, 31.80, 29.70, 27.60, 26.83, 26.33, 24.94, 23.83, 23.19, 16.47, 16.28, 14.03, 7.59. HR-MS (m/z) (ESI): calcd for $C_{54}H_{63}ClN_5O_{10}P$ $[M+H]^+$: 1008.4079; found: 1008.4038. Purity: 95.36% (by HPLC), t_R = 7.826 min.

Compound **9d**. 53 mg, yield: 71.0%. ^{1}H NMR (600 MHz, $CDCl_3$) δ 8.14 (d, *J* = 9.7 Hz, 1H), 7.79 (d, *J* = 3.4 Hz, 1H), 7.58 – 7.56 (m, 1H), 7.43 – 7.41 (m, 2H), 7.31 (d, *J* = 7.1 Hz, 2H), 7.14

(s, 1H), 6.90 (d, *J* = 6.4 Hz, 2H), 6.45 (d, *J* = 7.9 Hz, 2H), 5.65 (d, *J* = 17.0 Hz, 1H), 5.38 (d, *J* = 17.0 Hz, 1H), 5.21 (d, *J* = 4.1 Hz, 2H), 4.75 – 4.63 (m, 2H), 4.49 (d, *J* = 11.7 Hz, 1H), 4.39 (d, *J* = 11.9 Hz, 1H), 4.11 – 4.06 (m, 2H), 3.89 – 3.94 (m, 1H), 3.78 – 3.74 (m, 1H), 3.13 – 3.06 (m, 3H), 2.96 – 2.80 (m, 5H), 2.50 – 2.48 (m, 2H), 2.43 – 2.36 (m, 2H), 2.25 – 2.17 (m, 2H), 2.12 – 2.09 (m, 2H), 1.98 – 1.71 (m, 8H), 1.60 – 1.46 (m, 2H), 1.37 (t, *J* = 7.6 Hz, 3H), 1.26 – 1.24 (m, 3H), 1.14 (t, *J* = 6.8 Hz, 3H), 0.93 (t, *J* = 7.3 Hz, 3H). ^{13}C NMR (151 MHz, $CDCl_3$) δ 172.54, 167.65, 157.37, 153.02, 151.53, 150.24, 147.13, 146.74, 146.03, 145.40, 144.20, 144.10, 135.21, 131.69, 131.57, 131.31, 129.51, 129.30, 127.54, 127.12, 125.86, 121.78, 120.01, 114.66, 113.94, 95.90, 75.71, 67.10, 63.51, 63.35, 62.81, 56.22, 55.22, 50.12, 49.28, 43.99, 43.63, 33.81, 32.93, 31.80, 29.70, 27.49, 26.71, 26.33, 24.72, 23.70, 23.19, 16.46, 16.28, 14.04, 7.60. HR-MS (m/z) (ESI): calcd for $C_{54}H_{63}BrN_5O_{10}P$ $[M+H]^+$: 1052.3574; found: 1052.3546. Purity: 95.65% (by HPLC), t_R = 10.542 min.

Compound **9e**. 49 mg, yield: 69.0%. ^{1}H NMR (400 MHz, $CDCl_3$) δ 8.17 (d, *J* = 6.4 Hz, 1H), 7.83 (d, *J* = 1.8 Hz, 1H), 7.59 – 7.57 (m, 1H), 7.34 (d, *J* = 6.6 Hz, 2H), 7.14 (s, 1H), 6.90 (d, *J* = 8.2 Hz, 2H), 6.83 (d, *J* = 6.8 Hz, 2H), 6.49 (d, *J* = 8.2 Hz, 2H), 5.65 (d, *J* = 17.1 Hz, 1H), 5.39 (d, *J* = 17.1 Hz, 1H), 5.22 (d, *J* = 4.7 Hz, 2H), 4.74 – 4.58 (m, 2H), 4.47 (d, *J* = 12.1 Hz, 1H), 4.38 (d, *J* = 11.8 Hz, 1H), 4.15 – 4.03 (m, 2H), 3.93 – 3.87 (m, 1H), 3.74 (s, 3H), 3.69 – 3.63 (m, 1H), 3.14 – 3.04 (m, 3H), 2.93 – 2.73 (m, 5H), 2.49 (t, *J* = 7.1 Hz, 2H), 2.43 – 2.36 (m, 2H), 2.27 – 2.22 (m, 2H), 2.14 – 2.03 (m, 2H), 1.87 – 1.77 (m, 8H), 1.61 – 1.46 (m, 2H), 1.37 (t, *J* = 7.5 Hz, 3H), 1.27 – 1.24 (m, 3H), 1.11 (t, *J* = 7.0 Hz, 3H), 0.94 (t, *J* = 7.3 Hz, 3H). ^{13}C NMR (150 MHz, $CDCl_3$) δ 172.56, 167.64, 159.21, 157.37, 153.04, 151.50, 150.30, 147.12, 146.75, 146.03, 145.37, 144.55, 144.45, 131.57, 130.94, 129.21, 128.92, 127.70, 127.53, 127.10, 125.89, 119.97, 114.62, 113.98, 95.90, 75.69, 67.09, 63.26, 63.22, 62.62, 55.97, 55.22, 54.97, 50.11, 49.28, 44.11, 43.76, 33.84, 32.96, 31.80, 29.69, 27.68, 26.94, 26.33, 25.12, 23.95, 23.18, 16.48, 16.29, 14.03, 7.59. HR-MS (m/z) (ESI): calcd for $C_{55}H_{66}N_5O_{11}P$ $[M+H]^+$: 1004.4575; found:1004.4547. Purity: 97.65% (by HPLC), t_R = 8.005 min.

Compound **9f**. 46 mg, yield: 65.7%. ^{1}H NMR (400 MHz, $CDCl_3$) δ 8.17 (d, *J* = 9.1 Hz, 1H), 7.83 (d, *J* = 2.4 Hz, 1H), 7.60 – 7.56 (m, 1H), 7.32 – 7.30 (m, 2H), 7.14 (s, 1H), 7.11 – 7.09 (m, 2H), 6.90 (d, *J* = 8.3 Hz, 2H), 6.49 (d, *J* = 8.4 Hz, 2H), 5.66 (d, *J* = 17.2 Hz, 1H), 5.39 (d, *J* = 17.2 Hz, 1H), 5.22 (d, *J* = 4.7 Hz, 2H), 4.72 – 4.63 (m, 2H), 4.48 (d, *J* = 12.8 Hz, 1H), 4.39 (d, *J* = 11.7

Hz, 1H), 4.13 – 4.03 (m, 2H), 3.97 – 3.87 (m, 1H), 3.73 – 3.63 (m, 1H), 3.16 – 3.05 (m, 3H), 2.94 – 2.74 (m, 5H), 2.49 (t, *J* = 7.1 Hz, 2H), 2.45 – 2.34 (m, 2H), 2.28 (s, 3H), 2.22 – 2.01 (m, 4H), 1.87 – 1.83 (m, 2H), 1.78 – 1.72 (m, 6H), 1.57 – 1.47 (m, 2H), 1.38 (t, *J* = 7.4 Hz, 3H), 1.26 – 1.24 (m, 3H), 1.11 (t, *J* = 7.1 Hz, 3H), 0.94 (t, *J* = 7.5 Hz, 3H). ^{13}C NMR (100 MHz, $CDCl_3$) δ 172.30, 167.37, 157.15, 152.81, 151.31, 150.09, 146.93, 146.53, 145.81, 145.11, 144.41, 144.27, 137.31, 132.57, 131.39, 130.71, 129.07, 128.98, 127.51, 127.31, 126.88, 125.61, 119.80, 114.37, 113.75, 95.64, 75.47, 66.87, 63.02, 62.95, 62.47, 56.46, 54.95, 49.94, 49.03, 43.88, 43.54, 33.62, 32.75, 31.59, 29.45, 27.50, 26.73, 26.09, 24.90, 23.73, 22.93, 20.90, 16.23, 16.02, 13.77, 7.34. HR-MS (m/z) (ESI): calcd for $C_{55}H_{66}N_5O_{10}P$ $[M+H]^+$: 988.4625; found: 988.4600. Purity: 98.42% (by HPLC), t_R = 9.271 min.

Compound **9g**. 54 mg, yield: 77.1%. ^{1}H NMR (600 MHz, $CDCl_3$) δ 8.18 (d, *J* = 8.1 Hz, 1H), 7.85 (d, *J* = 2.2 Hz, 1H), 7.61 – 7.58 (m, 1H), 7.31 – 7.27 (m, 1H), 7.25 – 7.17 (m, 2H), 7.17 (s, 1H), 6.94 – 6.90 (m, 3H), 6.51– 6.49 (m, 2H), 5.67 (d, *J* = 17.0 Hz, 1H), 5.41 (d, *J* = 17.0 Hz, 1H), 5.24 (d, *J* = 4.1 Hz, 2H), 4.76 – 4.69 (m, 2H), 4.51 (d, *J* = 12.5 Hz, 1H), 4.42 (d, *J* = 12.4 Hz, 1H), 4.15 – 4.07 (m, 2H), 4.00 – 3.95 (m, 1H), 3.80 – 3.74 (m, 1H), 3.17 – 3.08 (m, 3H), 2.96 – 2.81 (m, 5H), 2.52 (t, *J* = 7.3 Hz, 2H), 2.47 – 2.39 (m, 2H), 2.28 – 2.08 (m, 4H), 1.90 – 1.72 (m, 8H), 1.61 – 1.51 (m, 2H), 1.39 (t, *J* = 7.9 Hz, 3H), 1.29 – 1.27 (m, 3H), 1.15 (t, *J* = 7.0 Hz, 3H), 0.96 (t, *J* = 7.3 Hz, 3H). ^{13}C NMR (150 MHz, $CDCl_3$) δ 172.53, 167.63, 163.75, 162.10, 157.36, 153.01, 151.50, 150.25, 147.11, 146.72, 146.02, 145.38, 144.24, 144.15, 138.90, 131.57, 131.29, 130.08, 129.28, 127.52, 127.10, 125.85, 123.52, 119.98, 114.95, 114.80, 114.63, 113.89, 95.90, 75.69, 67.08, 63.58, 63.37, 62.66, 56.37, 55.37, 50.01, 49.27, 44.01, 43.66, 33.82, 32.95, 31.79, 29.68, 27.48, 26.69, 26.32, 24.76, 23.74, 23.17, 16.43, 16.22, 14.02, 7.58. HR-MS (m/z) (ESI): calcd for $C_{54}H_{63}FN_5O_{10}P$ $[M+H]^+$: 992.4375; found: 992.4344. Purity: 95.74% (by HPLC), t_R = 9.434 min.

Compound **9h**. 47 mg, yield: 65.7%. ^{1}H NMR (600 MHz, $CDCl_3$) δ 8.16 (d, *J* = 8.6 Hz, 1H), 7.85 (d, *J* = 2.2 Hz, 1H), 7.59 – 7.57 (m, 1H), 7.43 (s, 1H), 7.33 (d, *J* = 7.0 Hz, 1H), 7.24 – 7.20 (m, 2H), 7.14 (s, 1H), 6.91 (d, *J* = 7.5 Hz, 2H), 6.47 (d, *J* = 8.1 Hz, 2H), 5.65 (d, *J* = 17.0 Hz, 1H), 5.39 (d, *J* = 17.0 Hz, 1H), 5.22 (d, *J* = 4.1 Hz, 2H), 4.71 – 4.64 (m, 2H), 4.47 (d, *J* = 12.5 Hz, 1H), 4.37 (d, *J* = 12.5 Hz, 1H), 4.13 – 4.05 (m, 2H), 3.99 – 3.92 (m, 1H), 3.78– 3.72 (m, 1H), 3.15 – 3.05 (m, 3H), 2.92 – 2.71 (m, 5H), 2.50 (t, *J* = 7.4 Hz, 2H), 2.45 – 2.47 (m, 2H), 2.26 – 2.02 (m, 4H), 1.88 – 1.83 (m, 2H), 1.75 – 1.61 (m, 6H), 1.57 – 1.46 (m, 2H), 1.37 (t, *J* = 7.6 Hz, 3H), 1.26

– 1.24 (m, 3H), 1.13 (t, *J* = 7.0 Hz, 3H), 0.94 (t, *J* = 7.3 Hz, 3H). ^{13}C NMR (150 MHz, $CDCl_3$) δ 172.52, 167.63, 157.35, 153.04, 151.48, 150.30, 147.10, 146.73, 145.99, 145.35, 144.19, 144.09, 138.39, 134.45, 131.55, 131.31, 129.83, 129.30, 128.10, 127.90, 127.08, 125.97, 125.88, 119.99, 114.61, 113.87, 95.88, 75.69, 67.09, 63.49, 63.39, 62.62, 56.34, 55.35, 50.16, 49.26, 44.14, 43.80, 33.81, 32.94, 31.79, 29.68, 27.78, 27.03, 26.31, 25.27, 24.03, 23.16, 16.43, 16.20, 14.01, 7.58. HR-MS (m/z) (ESI): calcd for $C_{54}H_{63}ClN_5O_{10}P$ $[M+H]^+$: 1008.4079; found: 1008.4048. Purity: 97.63% (by HPLC), t_R = 9.835 min.

Compound **9i**. 55 mg, yield: 73.7%. ^{1}H NMR (600 MHz, $CDCl_3$) δ 8.16 (d, *J* = 9.1 Hz, 1H), 7.81 (d, *J* = 2.2 Hz, 1H), 7.57 (d, *J* = 10.0 Hz, 2H), 7.37 – 7.32 (m, 2H), 7.18 – 7.15 (m, 1H), 7.14 (s, 1H), 6.91 (d, *J* = 7.2 Hz, 2H), 6.47 – 6.45 (m, 2H), 5.65 (d, *J* = 17.0 Hz, 1H), 5.38 (d, *J* = 17.0 Hz, 1H), 5.21 (d, *J* = 3.5 Hz, 2H), 4.71 – 4.63 (m, 2H), 4.50 (d, *J* = 12.5 Hz, 1H), 4.41 (d, *J* = 12.3 Hz, 1H), 4.12 – 4.05 (m, 2H), 3.97 – 3.92 (m, 1H), 3.78 – 3.70 (m, 1H), 3.14 – 3.07 (m, 3H), 2.96 – 2.88 (m, 5H), 2.49 (t, *J* = 7.4 Hz, 2H), 2.45 – 2.36 (m, 2H), 2.29 – 2.19 (m, 2H), 2.14 – 2.09 (m, 2H), 1.86 – 1.74 (m, 8H), 1.62 – 1.50 (m, 2H), 1.36 (t, *J* = 7.6 Hz, 3H), 1.26 – 1.24 (m, 3H), 1.13 (t, *J* = 6.9 Hz, 3H), 0.93 (t, *J* = 7.4 Hz, 3H). ^{13}C NMR (150 MHz, $CDCl_3$) δ 172.54, 167.64, 157.38, 153.05, 151.56, 150.21, 147.16, 146.76, 146.04, 145.41, 144.23, 144.13, 138.71, 131.62, 131.35, 131.01, 130.79, 130.15, 129.32, 127.54, 127.14, 126.44, 125.82, 122.66, 120.00, 114.68, 113.91, 95.90, 75.72, 67.10, 63.52, 63.43, 62.98, 56.33, 55.34, 50.09, 49.28, 43.85, 43.49, 33.84, 32.98, 31.80, 29.69, 27.25, 26.47, 26.34, 24.27, 23.41, 23.18, 16.44, 16.22, 14.03, 7.59. HR-MS (m/z) (ESI): calcd for $C_{54}H_{63}BrN_5O_{10}P$ $[M+H]^+$: 1052.3574; found: 1052.3536. Purity: 98.96% (by HPLC), t_R = 8.274 min.

Compound **9j**. 43 mg, yield: 60.5%. ^{1}H NMR (600 MHz, $CDCl_3$) δ 8.17 (d, *J* = 8.8 Hz, 1H), 7.83 (d, *J* = 2.3 Hz, 1H), 7.60 – 7.57 (m, 1H), 7.23 – 7.21 (m, 1H), 7.15 (s, 1H), 7.03 – 6.99 (m, 2H), 6.91 (d, *J* = 8.3 Hz, 2H), 6.78 (d, *J* = 6.80 Hz, 1H), 6.50 (d, *J* = 8.2 Hz, 2H), 5.66 (d, *J* = 17.0 Hz, 1H), 5.39 (d, *J* = 17.0 Hz, 1H), 5.23 (d, *J* = 4.8 Hz, 2H), 4.70 – 4.65 (m, 2H), 4.47 (d, *J* = 12.8 Hz, 1H), 4.38 (d, *J* = 12.3 Hz, 1H), 4.15 – 4.05 (m, 2H), 3.95 – 3.91 (m, 1H), 3.70 (s, 3H), 3.70 – 3.61 (m, 1H), 3.16 – 3.05 (m, 3H), 2.92 – 2.70 (m, 5H), 2.49 (t, *J* = 7.1 Hz, 2H), 2.46 – 2.37 (m, 2H), 2.27 – 2.02 (m, 4H), 1.89 – 1.85 (m, 2H), 1.81 – 1.60 (m, 6H), 1.56 – 1.44 (m, 2H), 1.38 (t, *J* = 7.7 Hz, 3H), 1.28 – 1.25 (m, 3H), 1.12 (t, *J* = 7.0 Hz, 3H), 0.94 (t, *J* = 7.5 Hz, 3H). ^{13}C NMR (150 MHz, $CDCl_3$) δ 172.54, 167.62, 159.73, 157.37, 153.05, 151.50, 150.31, 147.06, 146.73,

146.00, 145.33, 144.54, 144.44, 137.61, 131.58, 131.03, 129.54, 129.22, 127.52, 127.08, 125.88, 120.20, 120.02, 114.59, 113.92, 113.46, 113.32, 95.89, 75.68, 67.09, 63.31, 63.27, 62.59, 56.74, 55.74, 55.21, 50.17, 49.26, 44.19, 43.84, 33.83, 32.96, 31.81, 29.69, 27.85, 27.09, 26.33, 25.39, 24.12, 23.17, 16.46, 16.24, 14.02, 7.58. HR-MS (m/z) (ESI): calcd for $C_{55}H_{66}N_5O_{11}P$ $[M+H]^+$: 1004.4575; found:1004.4545. Purity: 98.01% (by HPLC), t_R = 8.853 min.

4.2. In vitro cytotoxicity.

In this study, all human cancer cell lines including A549 (lung), MCF-7 (breast), MG-63 (osteosarcoma), U2OS (osteosarcoma), SK-OV-3 (ovarian) and SK-OV-3/CDDP (cisplatin resistance cells) cancer cell lines using MTT assay were purchased from the Shanghai Cell Bank of the Chinese Academy of Sciences. Culture medium Roswell Park Memorial Institute (RPMI-1640), phosphate buffered saline (PBS, pH=7.2), fetal bovine serum (FBS), and Antibiotice-Antimycotic came from KeyGen Biotech Company (China). Cells were cultivate in the supplemented with 10% FBS, 100 units/ml of penicillin and 100 g/ml of streptomycin in a humidified atmosphere of 5% CO_2 at 37 ^oC. Tested compounds were dissolved to stock concentrations of 2 mM with DMSO (Sigma); the positive drug Ir was served as a positive control, and the cytotoxicity of all target compounds against the tested cancer cells was also investigated using MTT assay. All data were independently tested repeated in triplicate.

*4.3 HPLC analyses on the stability of compound **9b***.

The stability of compound **9b** dissolved in PBS (pH 7.4) with or without 10% FBS examined by analyzing concentration of 0.1 mg/mL, and the sample was stored at 37°C for 12 and 24 h, separately. Reversed-phase HPLC was carried out on a 4.6×250 mm ODS column. HPLC profiles were recorded on UV detection at 254 nm. Mobile phase consisted of Methanol/Water (0.1% TFA)/Water (50:50-100:0, v/v), and flow rate was 1.0 mL/min. The samples were taken for HPLC analysis after filtered by 0.45 μm filter.

4.4. Topo I inhibitory activity.

Western blot analysis was performed as described previously [45]. Firstly, the supercoiled pBR322 DNA (TaKaRa, Kyoto, Japan) was measured to reflect inhibition of the Topo I (TaKaRa, Kyoto, Japan) catalytic ability by test compound **9b**, and the Ir was served as a positive drug. Secondly, the reaction solution was prepared according to the supplier's instructions, and incubated at 37 ^oC for 30 min. A dye solution containing 40% glycerol, 0.25% xylene cyanol ff

and 0.25% bromophenol blue was added to end the reaction. Finally, the mixtures were added to 1% agarose gel and subjected to electrophoresis for 40 min in 1 TAE buffer (40 mM Tris-acetate, 2 mM EDTA and 19.9 mM AcHO, respectively), and then the gels were stained with 200 mL 1 X TAE buffer containing 5 mg/mL EB for 30 min, and washed for 20 min in 200 mL 1 TAE buffer. Finally, Ethidium bromide stained agarose gel was photographed using Gel Doc XR (Bio-Rad).

4.5. Anti-tumor activity in vivo.

The *in vivo* cytotoxic activity of **9b** was further investigated by human ovarian cells (SK-OV-3) in BALB/c nude mice. Five-week-old female BALB/c nude mice were purchased from Shanghai Ling Chang biotechnology company (China); tumors were induced by a subcutaneous injection in their dorsal region of 1.0×10^7 cells in 100 mL of sterile PBS. Animals were randomly divided into four groups, and started on the second day. When the tumors reached a volume of 100-150 mm^3 in all mice on day 18, the first group was injected with an equivalent volume of 5% dextrose via a tail vein as the vehicle control mice. No. 2 and No. 3 groups were treated with **9b** at doses of 10 mg/kg and 20 mg/kg once a week for three weeks, respectively. No. 4 group was treated with Ir at the dose of 20 mg/kg once a week for three weeks. All tested compounds were dissolved in vehicle. Tumor volume and body weight were recorded every other day after drug treatment. We collected and weighed the tumors and calculated the inhibition rate of tumor growth (IRT) at the end of treatment. All mice were sacrificed after three weeks of treatment and the tumor volumes were measured with electronic digital calipers and determined by measuring length (A) and width (B) to calculate volume ($V = AB^2/2$).

4.6. H&E staining.

Tumor samples were shown in routine histopathological examination using Hematoxylin and Eosin (H&E) staining. Firstly, mouse organs including liver, heart, lung, kidney and spleen were collected in 4% paraformaldehyde for proper fixation and then embedded in paraffin using tissue embedding machine. Secondly, sections were cut and stained with H&E, and then sections were prepared orderly by dewaxing, stainingm and dehydration. The sections were stained in eosin-phloxine solution for 1 min after staining in Harris hematoxylin solution, and then dehydrated and mounted with neutral resin. Finally, the tissue morphology was then imaged by fluorescence microscopy.

4.7. Cell apoptosis assay.

Firstly, SK-OV-3 were gromn in each well of six-well plates at the density of 5.0×10^5 cells/mL of the RPMI-1640 medium with 10% FBS to the final volume of 2 mL. Secondly, after cells incubated for overnight, then cells treated with **9b** (5.0 or 10 μM) and Ir (10 μM) for 24 h. After 24 h incubation, cells were collected, washed thrice in PBS, and re-suspended in 120 μL of binding buffer at a final concentration of 0.5×10^6 cells/mL, and then cells were treated with 5 μL of annexin V-FITC and 5 μL of PI in the dark at 4 °C for 30 min, respectively. Finally, the sample was analyzed by flow cytometer.

4.8. Cell morphological assay.

Firstly, SK-OV-3 cells were grown in each well of six-well plates at the density of 5.0×10^4 cells/mL of the RPMI-1640 medium with 10% FBS to the final volume of 2 mL. Secondly, cells treated with **9b** (5.0 or 10 μM) and Ir (10 μM) for 24 h. After 24 h treatment, the cells were washed twice with ice-cold PBS, and incubated with calcein AM and PI for 30 min. Finally, cells were visualized by fluorescence microscope after incubation of 30 min.

4.9. Cell wound-healing assay.

Firstly, SK-OV-3 cells were grown in 6-well plates and allowed to grow to ≥ 95% confluent. The wounds were created perpendicular to the lines by 20 μL tips, and then unattached cells were removed by washing with twice in ice-cold PBS. Secondly, cells treated with **9b** (5.0 or 10 μM) and Ir (10 μM) for 24 h. After 24 h incubation, the cells were washed twice with ice-cold PBS, and then photographed to mark the final scratched tracks. Finally, the migration rates analyzed by Equation 1: Migration rate (%) = (d1-d2)/d1, and the d1 and 2 represented the width of wound at 0 and 24 h, respectively.

4.10. Cell cycle assay.

Firstly, SK-OV-3 cells were grown in each well of six-well plates at the density of 5×10^5 cells/mL of the RPMI-1640 medium with 10% FBS to the final volume of 2 mL. Secondly, after cells incubated for overnight, then cells treated with **9b** (5.0 or 10 μM) and Ir (10 μM) for 24 h. After 24 h incubation, cells were collected, washed twice in PBS, fixed with ice-cold 70% ethanol at -20 °C for overnight. The cells were treated with 100 μg /mL RNase A for 30 min at 37 °C after washed twice in PBS. Finally, cells stained with PI at 1 mg/ml in the dark at 4 °C for 30 min analyzed by flow cytometry.

4.11. Mitochondrial membrane potential (MMP) assay.

Firstly, SK-OV-3 cells were grown in each well of six-well plates at the density of 5.0×10^4 cells/mL of the RPMI-1640 medium with 10% FBS to the final volume of 2 mL. Secondly, after cells incubated for overnight, then cells treated with **9b** (5.0 or 10 μM) and Ir (10 μM) for 24 h. After 24 h incubation, cells were then stained with 2 μM JC-1 in the dark at room temperature for 30 min. Finally, cells were harvested at 2000 rpm and washed thrice in PBS analyzed by flow cytometry after 30 min of incubation.

4.12. Reactive oxygen species (ROS) assay.

Firstly, SK-OV-3 cells were grown in each well of six-well plates at the density of 5.0×10^4 cells/mL of the RPMI-1640 medium with 10% FBS to the final volume of 2 mL. Secondly, after cells incubated for overnight, then cells treated with **9b** (5.0 or 10 μM) and Ir (10 μM) for 24 h. After 24 h incubation, cells were then stained with DCFH-DA in the dark at 37 °C for 30 minutes. Finally, cells were harvested at 2000 rpm and washed thrice in PBS analyzed by flow cytometry after 30 min of incubation.

4.13. Western blot assay.

Western blot analysis was performed as described previously [38]. Firstly, SK-OV-3 cells were grown in each well of six-well plates at the density of 1.0×10^5 cells/mL of the RPMI-1640 medium with 10% FBS to the final volume of 2 mL. Secondly, after cells incubated for overnight, then cells treated with **9b** (5.0 or 10 μM) and Ir (10 μM) for 24 h. After treatment, cells were collected, centrifuged, and washed thrice in ice-cold PBS. The pellet was then re-suspended in lysis buffer containing 150 mM NaCl, 50 mM Tris (pH 7.4), 1% (w/v) sodium deoxycholate, 1% (v/v) Triton X-100, 0.1% (w/v) SDS, and 1 mM EDTA (Beyotime, China). The lysates were incubated at 37 °C for 30 min, and centrifuged at 20000g at 4 °C for 10 min, and then the protein concentration in the supernatant was detected by the BCA protein assay reagents. Presently, equal amounts of protein per line were was separated on 12% SDS polyacrylamide gel electrophoresis and transferred to PVDF Hybond-P membrane (GE Healthcare). Membranes were incubated with 5% skim milk in Tris-buffered saline with Tween 20 (TBST) buffer for 1 h and then the membranes being gently rotated overnight at 4 °C. Membranes were then incubated with primary antibodies against Bcl-2, Bax, caspase-3 and -9 or GAPDH for overnight at 4 °C. After three washes in TBST, then the membranes were next incubated with peroxidase labeled secondary antibodies for 2 h. Finally, all membranes were washed with TBST four times for 20 minutes and

the protein blots were analyzed by chemiluminescence reagent (Thermo Fischer Scientifics Ltd.). The X-ray films were developed with developer and fixed with fixer solution.

Notes

The authors declare no competing financial interest.

Acknowledgments

Firstly, we are grateful to the National Natural Science Foundation of China (Grant Nos. 21977021, 81760626 and 81760626), and the Ministry of Education Innovation Team Fund (IRT_16R15, 2016GXNSFGA380005). Secondly, we would like to thank the Natural Science Foundation of Guangxi Province (AB17292075) and Guangxi Funds for Distinguished Experts. Finally, we are also very grateful to the Key University Science Research Project of Jiangsu Province (18KJA360001) and the National Science Foundation of the Jiangsu Higher Education Institutions of China (19KJA150008) and the Open Project Program of the Jiangsu Key Laboratory of Regional Resource Exploitation and Medicinal Research (Grant Nos. LPRK201805 and LPRK201902) and the Major projects of natural science research in Colleges and universities of Jiangsu Province (18KJA530002).

References

[1] R. L. Siegel, K. D. Miller and A. Jemal, Cancer statistics, 2015. Ca-Cancer J. Clin. 65 (2015) 5-29.

[2] Y.T. Wang, Y.J. Qin, N. Yang, Y. L. Zhang, C.H. Liu, H.L. Zhu, Synthesis, biological evaluation, and molecular docking studies of novel 1-benzene acyl-2-(1-methylindol-3-yl)-benzimidazole derivatives as potential tubulin polymerization inhibitors, Eur. J. Med. Chem. 99 (2015) 125-137.

[3] Y. Gou, J. Wang, S.F. Chen, Z. Zhang, Y. Zhang, W. Zhang, F. Yang, a Nheterocyclic thiosemicarbazone Fe(III) complex: Characterization of its antitumor activity and identification of anticancer mechanism, Eur. J. Med. Chem. 123 (2016) 354-364.

[4] J. Shi, P.W. Kantoff, R. Wooster, O.C. Farokhzad, Cancer nanomedicine: progress, challenges and opportunities, Nat. Rev. Cancer. 17 (2016) 20-37.

[5] Q. Mou, Y. Ma, X. Zhu, D. Yan, A small molecule nanodrug consisting of amphiphilic targeting ligand-chemotherapy drug conjugate for targeted cancer therapy, J. Controlled Release.230 (2016) 34-44.

[6] D.V. Santi, E.L. Schneider, and G.W. Ashley, Macromolecular prodrug that provides the irinotecan (CPT-11) active-metabolite SN-38 with ultralong half-life, low cmax , and low glucuronide formation, J. Med. Chem. 57 (2014) 2303-2314.

[7] N.H. Oberlies, D.J. Kroll, Camptothecin and taxol: historic achievements in natural products research, J. Nat. Prod. 67 (2004) 129-135.

[8] Wang, H.K.; Morris-Natschke, S. L.; Lee, K. H. Antitumor agents 170. Recent advances in the discovery and development of topoisomerase inhibitors as antitumor agents, Med. Res. Rev. 17 (1997) 367-425.

[9]. X. Zhang, K.Y. Tang, H. Wang, Y.Q. Liu, B. Bao, Y.F. Fang, X.W. Zhang, and W. Lu, Design, synthesis, and biological evaluation of new cathepsin B-sensitive camptothecin nanoparticles equipped with a novel multifuctional linker, Bioconjugate Chem. 27 (2016) 1267-1275.

[10] T. Conroy, F. Desseigne, M. Ychou, O. Bouche, R. Guimbaud, Y. Becouarn, A. Adenis, J.L. Raoul, S. Gourgou-Bourgade,; C. delaFouchardiere, J. Bennouna, J.B. Bachet, F. Khemissa-Akouz, D. Pere´-Verge´, C. Delbaldo, E. Assenat, B. Chauffert, P. Michel, C. Montoto-Grillot, M. Ducreux, FOLFIRINOX versus gemcitabine for metastatic pancreatic cancer, N. Engl. J. Med. 364 (2011) 1817-1825.

[11] X.S. Liu, A. Situ, Y.N. Kang, K.R. Villabroza, Y.P. Liao, C.H. Chang, T. Donahue, A.E. Nel, and H. Meng, Irinotecan delivery by lipid-coated mesoporous silica nanoparticles shows improved efficacy and safety over liposomes for pancreatic cancer, ACS Nano. 10 (2016) 2702-2715.

[12] Hecht, J. R. Gastrointestinal toxicity of irinotecan. Oncology 12 (1998) 72-78.

[13] F. Loupakis, M. Schirripa, C. Caparello, N. Funel, L. Pollina, E. Vasile, C. Cremolini, L. Salvatore, M.; Morvillo C. Antoniotti, Histopathologic evaluation of liver metastases from colorectal cancer in patients treated with FOLFOXIRI plus bevacizumab, Br. J. Cancer. 108 (2013) 2549-2556.

[14] R.H. Mathijssen, R.J. van Alphen, J. Verweij, W.J. Loos, K. Nooter, G. Stoter, A. Sparreboom, Clinical pharmacokinetics and metabolism of irinotecan (CPT-11), Clin. Cancer Res. 27 (2001) 2182-2194.

[15] Y.Q. Huang, J.D. Yuan, H.F. Ding, Y.S. Song, G. Qian, J.L. Wang, M. Ji, Y. Zhang, Design, synthesis and pharmacological evaluation of a novel PEG-cRGD-conjugated irinotecan

derivative as potential antitumor agent, Eur. J. Med. Chem. 158 (2018) 82-90.

[16] X.S Liu, J.H. Jiang, R. Chan, Y. Ji, J.Q. Lu, Y.P. Liao, M. Okene, J. Lin, P. Lin, C.H. Chang, X. Wang, I. Tang, E. Zheng, W. Qiu, Z.A. Wainberg, A.E. Nel, and H. Meng, Improved efficacy and reduced toxicity using a custom-designed irinotecan-delivering silicasome for orthotopic colon cance, ACS Nano. 13 (2019) 38-53.

[17] D.C. Drummond, C.O. Noble, Z. Guo, K. Hong, J.W. Park, D.B. Kirpotin, Development of a highly active nanoliposomal irinotecan using a novel intraliposomal stabilization strategy. Cancer Res. 66 (2006) 3271-3277.

[18] J. Li, F. Liu, S. Gupta, C. Li, Interventional nanotheranostics of pancreatic ductal adenocarcinoma, Theranostics. 6 (2016) 1393-1402.

[19] A. Khalid, S. Persano, H. Shen, Y. Zhao, E. Blanco, M. Ferrari, J. Wolfram, Strategies for improving drug delivery: Nanocarriers and microenvironmental priming, Expert Opin. Drug Delivery. 14 (2017) 865-877.

[20] K. Knop, R. Hoogenboom, D. Fischer, U.S. Schubert, Poly(Ethylene Glycol) in drug delivery: pros and cons as well as potential alternatives, Angew. Chem., Int. Ed. 49 (2010) 6288-6308.

[21] D. Yu, P. Peng, S.S. Dharap, Y. Wang, M. Mehlig, P. Chandna, H. Zhao, D. Filpula, K. Yang, V. Borowski, G. Borchard, Z. Zhang, T. Minko, Antitumor activity of poly(Ethylene Glycol)-camptothecin conjugate: The inhibition of tumor growth in vivo, J. Controlled Release. 110 (2005) 90-102.

[22] Y. Li, J.Y. Lin, J.Y. Ma, L. Song, H.R. Lin, B.W. Tang, D.Y. Chen, G.H. Su, S.F. Ye, X. Zhu, F.H. Luo, and Z.Q. Hou, Methotrexate-camptothecin prodrug nanoassemblies as a versatile nanoplatform for biomodal imaging-guided self-active targeted and synergistic chemotherapy, ACS Appl. Mater. Interfaces. 9 (2017) 34650-34665.

[23] K. Hochdörffer, K.A. Ajaj, C.S. Obodozie, and F. Kratz, Development of novel bisphosphonate prodrugs of doxorubicin for targeting bone metastases that are cleaved pH dependently or by cathepsin B: Synthesis, cleavage properties, and binding properties to hydroxyapatite as well as bone matrix, J. Med. Chem. 55 (2012) 7502-7515.

[24] N.J. Rahier, B.M. Eisenhauer, R. Gao, S.H. Jones, and S.M. Hecht, Water-soluble camptothecin derivatives that are intrinsic topoisomerase I poisons, Org. lett. 6 (2004) 321-324.

[25] X.C. Huang, R.Z. Huang, S.H. Gou, Z.M. Wang, and H.S. Wang, Anticancer platinum(IV) prodrugs containing monoaminophosphonate ester as a targeting group inhibit matrix metalloproteinases and reverse multidrug resistance, Bioconjugate Chem. 28 (2017) 1305-1323.

[26] E. Kotsikorou, E. Oldfield, A Quantitative Structure-Activity Relationship and Pharmacophore Modeling Investigation of Aryl-X and Heterocyclic Bisphosphonates as Bone Resorption Agents, J. Med. Chem. 46 (2003) 2932-2944.

[27 Xue, Z. Q., Lin, M., Zhu, J., Zhang, J., Li, Y. Z., and Guo, Z. J. Platinum(II) compounds bearing bone-targeting group: Synthesis, crystal structure and antitumor activity. Chem. Commun. 46 (2010) 1212-1214.

[28] K.B. Huang, Z.F. Chen, Y.C. Liu, ZQ. Li, J.H. Wei, M. Wang, X.L. Xie, and H. Liang, Platinum(II) complexes containing aminophosphonate esters: Synthesis, characterization, cytotoxicity and action mechanism, Eur. J. Med. Chem. 64 (2013) 554-561.

[29] F. Orsini, G. Sello, M. Sisti, Aminophosphonic acids and derivatives. Synthesis and biological applications, Curr. Med. Chem. 17 (2010) 264-289.

[30] X.C. Huang, M. Wang, Y.M. Pan, X.Y. Tian, H.S. Wang, Y. Zhang, Synthesis and antitumor activities of novel a-aminophosphonates dehydroabietic acid derivatives, Bioorgan. Med. Chem. Lett. 23 (2013) 5283-5289.

[31] L. Jin, B. Zhang, S.X. Hua, M. Ji, X.C Huang, R.Z. Huang, H.S. Wang, Glycyrrhetinic acid derivatives containing aminophosphonate ester species as multidrug resistance reversers that block the NF-κB pathway and cell proliferation, Bioorgan. Med. Chem. Lett. 28 (2018) 3700-3707.

[32] K.B. Huang, Z.F. Chen, Y.C. Liu, Z.Q. Li, J.H. Wei, M. Wang, G.H. Zhang, and H. Liang, Platinum(II) complexes with mono-aminophosphonate ester targeting group that induce apoptosis through G1 cell-cycle arrest: Synthesis, crystal structure and antitumor activity, Eur. J. Med. Chem. 63 (2013) 76-84.

[33] R. Sasanelli, A. Boccarelli, D. Giordano, M. Laforgia, F. Arnesano, G. Natile, C. Cardellicchio, M.A.M. Capozzi, and M. Coluccia, Platinum complexes can inhibit matrix metalloproteinase activity: Platinum-diethyl[(methylsulfinyl)methyl]-phosphonate complexes as inhibitors of matrix metalloproteinases 2,3, 9, and 12, J. Med. Chem. 50 (2007) 3434-3441.

[34] F. Arnesano, A. Boccarelli, D. Cornacchia, F. Nushi, R. Sasanelli, M. Coluccia, and G. Natile, Mechanistic insight into the inhibition of matrix metalloproteinases by platinum substrates, J. Med. Chem. 52 (2009) 7847-7855.

[35] L. Jin, B. Zhang, S. Hua, M. J, X. Huang, R. Huang, H. Wang, Glycyrrhetinic acid derivatives containing aminophosphonate ester species as multidrug resistance reversers that block the NF-κB pathway and cell proliferation, Bioorgan. Med. Chem. Lett. 28 (2018) 3700-3707.

[36] Sinha, K.; Das, J.; Pal, P. B.; Sil, P. C. Oxidative stress: the mitochondria-dependent and mitochondria-independent pathways of apoptosis, *Arch. Toxicol*. 87 (2013) 1157-1180.

[37] K.B. Huang, F.Y. Wang, X.M. Tang, H.W. Feng, Z.F. Chen,Y.C. Liu, Y.N. Liu, and H. Liang, Organometallic gold(III) complexes similar to tetrahydroisoquinoline induce ER-stress-mediated apoptosis and Pro-death autophagy in A549 cancer cells, J. Med. Chem. 61 (2018) 3478-3490.

[38] S.H. Huang, L.W. Wu, A.C. Huang, C.C. Yu, J.C. Lien, Y.P. Huang, J.S. Yang, J.H. Yang, Y.P. Hsiao, W.G. Wood, C.S. Yu, J.G. Chung, Benzyl isothiocyanate (BITC) induces G2/M phase arrest and apoptosis in human melanoma A375.S2 cells through reactive oxygen species (ROS) and both mitochondriadependent and death receptor-mediated multiple signaling pathways, J. Agric. Food Chem. 60 (2012) 665-675.

[39] H.U. Simon, A. Haj-Yehia, F. Levi-Schaffer, Role of reactive oxygen species (ROS) in apoptosis induction, Apoptosis. 5 (2000) 415-418.

[40] R.W.Y. Sun, C.N. Lok, T.T.H. Fong, C.K.L. Li, Z.F. Yang, T. Zou, A.F.M. Siu, C.M. Che, A dinuclear cyclometalated gold(III)-phosphine complex targeting thioredoxin reductase inhibits hepatocellular carcinoma *in vivo*, Chem.Sci. 4 (2013) 1979-1988.

[41] M.C. Wei, W.X. Zong, E.H.Y. Cheng, T. Lindsten, V. Panoutsakopoulou, A.J. Ross, K. A. Roth, G.R. MacGregor, C.B. Thompson, S.J. Korsmeyer, Proapoptotic Bax and Bak: a requisite gateway to mitochondrial dysfunction and death, Science. 292 (2001) 727-730.

[42] J.Yan, J. Chen, S. Zhang, J.H. Hu, L. Huang, and X.S. Li, Synthesis, evaluation, and mechanism study of novel indole-chalcone derivatives exerting effective antitumor activity through microtubule destabilization in vitro and in vivo, J. Med. Chem. 59 (2016) 5264-5283.

[43] P. Huang, D.L. Wang, Y. Su, W. Huang, Y.F Zhou, D. Cui,‡ X.Y. Zhu,and D.Y. Yan,

Combination of small molecule prodrug and nanodrug delivery: Amphiphilic drug-drug conjugate for cancer therapy, J. Am. Chem. Soc. 136 (2014) 11748-11756.

[44] S. Xu, H. Yao, S. Luo, Y.K. Zhang, D.H. Yang, D. Li, G. Wang, M. Hu, Y. Qiu, X. Wu, H. Yao, W. Xie, Z.S. Chen, and J. Xu, A novel potent anticancer compound optimized from a natural oridonin scaffold induces apoptosis and cell cycle arrest through the mitochondrial pathway, J. Med. Chem. 60 (2017) 1449-1468.

[45] W. Hou, Z.Y. Wang, C.K. Peng, J. Lin, X. Liu, Y.Q. Chang, J. Xu, R.W. Jiang, H. Lin, P.H. Sun, W.M. Chen, Novel securinine derivatives as topoisomerase I based antitumor agents, Eur. J. Med. Chem. 122 (2016) 149-163.

Scheme :

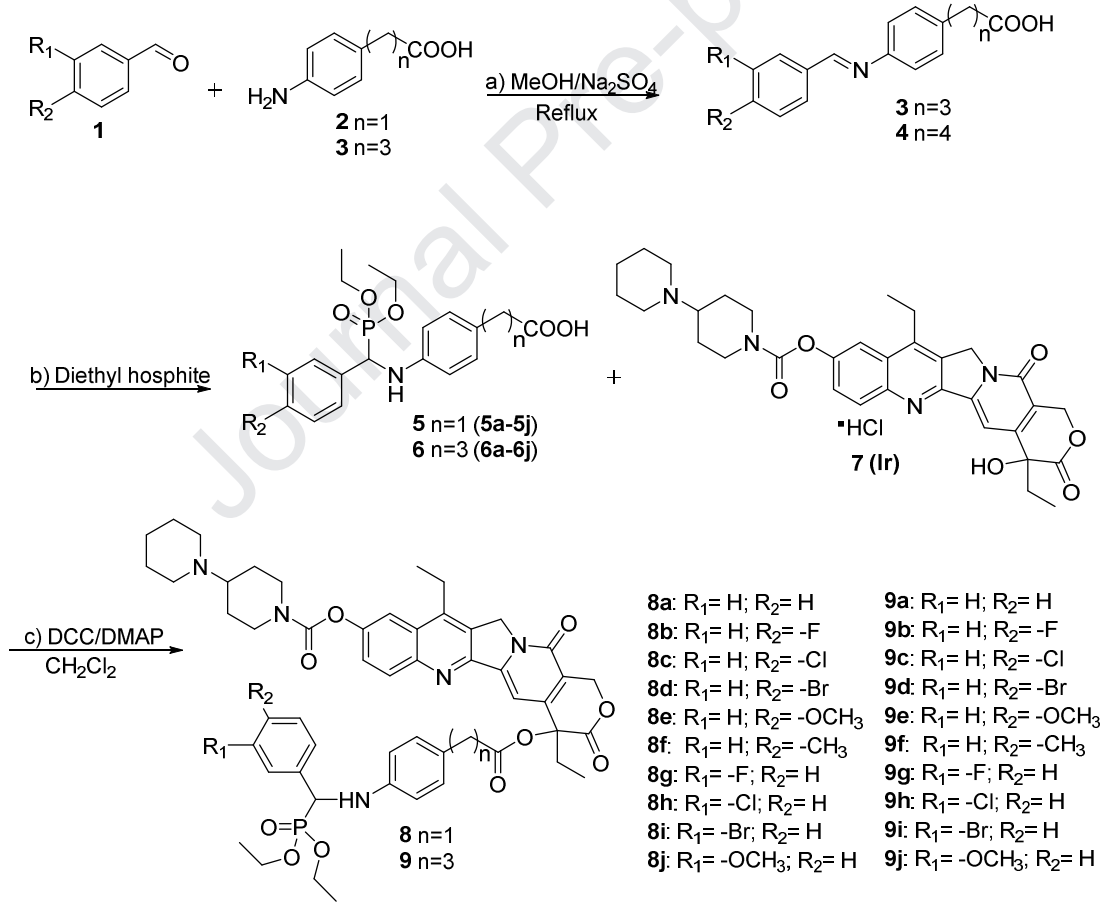

Scheme 1: Synthetic pathway to target compounds **8** and **9**. Reagents and conditions: (a) CH_3OH, reflux; (b) diethyl phosphite, 50 °C; (c) DCC, DMAP, CH_2Cl_2, 30 °C.

Highlights

- A novel series of Ir derivatives were synthesized as potential antitumor agents.
- **9b** exhibited stronger anticancer activity toward to human cancer cells compared to Ir.
- **9b** effectively arrested SK-OV-3 cells at S stage.
- **9b** exhibited antitumor efficacy in the SK-OV-3 xenograft model better than Ir.
- **9b** may induce SK-OV-3 cells apoptosis through mitochondrion pathways.

Declaration of interests

☒ The authors declare that they have no known competing financial interests or personal relationships that could have appeared to influence the work reported in this paper.

☐The authors declare the following financial interests/personal relationships which may be considered as potential competing interests: